EFFECT OF NANOFLUIDS ON HEAT TRANSFER CHARACTERISTICS OF A HEAT PIPE

AMIN KAMYAR

FACULTY OF ENGINEERING

UNIVERSITY OF MALAYA

KUALA LUMPUR

2013

EFFECT OF NANOFLUIDS ON HEAT TRANSFER CHARACTERISTICS OF A HEAT PIPE

AMIN KAMYAR

RESEARCH REPORT SUBMITTED IN PARTIAL FULFILLMENT OF THE REQUIREMENT FOR THE DEGREE OF MASTER OF MECHANICAL ENGINEERING

FACULTY OF ENGINEERING

UNIVERSITY OF MALAYA

KUALA LUMPUR

2013

ORIGINAL LITERARY WORK DECLARATION

Name of Candidate: **Amin Kamyar** (I.C/Passport No:)

Registration/Matric No: **KGH100027**

Name of Degree: **Master of Engineering (M.Eng.)**

Title of Project Paper/Research Report/Dissertation/Thesis ("this Work"):

EFFECT OF NANOFLUIDS ON HEAT TRANSFER CHARACTERISTICS OF A HEAT PIPE

Field of Study: **Energy**

I do solemnly and sincerely declare that:

(1) I am the sole author/writer of this Work;
(2) This Work is original;
(3) Any use of any work in which copyright exists was done by way of fair dealing and for permitted purposes and any excerpt or extract from, or reference to or reproduction of any copyright work has been disclosed expressly and sufficiently and the title of the Work and its authorship have been acknowledged in this Work;
(4) I do not have any actual knowledge nor do I ought reasonably to know that the making of this work constitutes an infringement of any copyright work;
(5) I hereby assign all and every rights in the copyright to this Work to the University of Malaya ("UM"), who henceforth shall be owner of the copyright in this Work and that any reproduction or use in any form or by any means whatsoever is prohibited without the written consent of UM having been first had and obtained;
(6) I am fully aware that if in the course of making this Work I have infringed any copyright whether intentionally or otherwise, I may be subject to legal action or any other action as may be determined by UM.

Candidate's Signature Date

Subscribed and solemnly declared before,

Witness's Signature Date

Name:

Designation:

This work is dedicated to my beloved family who has always confided in me and heartened me throughout all that I choose to pursue.

Acknowledgements

I would like to give all glory to almighty God for providing me the ability to accomplish this work. He has been the source of hope and strength in my life and has granted me with countless benevolent gifts.

I would like to express deep gratitude to Professor Dr. Saidur Rahman Abdul Hakim, for having faith in me to be able to achieve this accomplishment, for all his invaluable support during this research.

I would also like to extend my appreciation to Professor Dr. Ong Kok Seng from Monash University, Sunway Campus for his benign guidance and help throughout this investigation. Without his contribution, this research would not have been achievable.

Thanks are also extended to Mr. Jason Gan Jie Sheng and Mr. Christopher Lim for their valuable contribution during establishment of the test rig. They have been great friends and made the experiments possible to conduct.

Finally, I tend to take this opportunity to appreciate the indispensable and perpetual support from my father, mother and sister whose words have always instilled incentives in me during my life.

Abstrak

Thermosyphons digunakan secara meluas dalam aplikasi kejuruteraan haba seperti penyejukan elektronik dan bahan buangan terima kasih pemulihan haba kepada keupayaan penyejukan pasif mereka. Prestasi thermosyphons boleh diperbaiki dengan pelbagai cara salah satu yang berubah sifat-sifat dan ciri-ciri pengangkutan pemindahan haba bendalir kerja. Nanofluid, merujuk kepada penggantungan koloid cecair asas dan nanosized (1-100 nm) zarah pepejal, adalah satu pilihan untuk mencapai sasaran ini. Menggabungkan pertukaran sifat haba thermosyphons terma dan ciri-ciri yang berbeza nanofluids boleh membuka ufuk baru dalam bidang pemindahan haba. Kajian semasa menumpukan kepada prestasi terma yang thermosyphon tertutup dua fasa dipenuhi dengan dua nanofluids menggunakan air sebagai bendalir asas bercampur dengan Al_2O_3 dan $TiSiO_4$ nanopartikel. Nanofluids telah disediakan dalam kepekatan isipadu yang berbeza (0.01%, 0.02%, 0.05% dan 0.075) dan beban haba yang berbeza (40W, 70W, 120W, 180W dan 210W) telah disediakan di bahagian penyejat. Keputusan menunjukkan bahawa kedua-dua nanofluids meningkatkan prestasi melalui pengurangan rintangan haba sebanyak 65% (pada 0.05 vol.% Untuk Al_2O_3) dan 57% (pada 0.075 vol.%). Penambahbaikan lain yang juga didapati dalam bentuk peningkatan pekali pemindahan haba dan penurunan suhu dinding penyejat. Untuk semua cecair bekerja, pekali pemindahan haba meningkat dengan peningkatan dalam kuasa input. Kedua-dua nanofluids menyebabkan pemindahan haba kebangkitan pekali berbanding dengan air tulen. Nilai maksimum bagi pekali pemindahan haba berlaku pada 0.05 vol.% untuk nanopartikel alumina, manakala nilai ini berlaku pada 0,075 vol.% untuk $TiSiO_4$/water nanofluid. Taburan suhu sepanjang thermosyphon menunjukkan perubahan kerana pengurangan yang berlaku selepas menggunakan nanofluids sebagai bendalir kerja.

Abstract

Thermosyphons are widely used in thermal engineering application such as cooling of electronics and waste heat recovery thanks to their passive cooling ability. Performance of thermosyphons could be improved by various means like changing the transport properties and heat transfer characteristics of the working fluid. Nanofluid, referring to a colloidal suspension of a base fluid and nanosized (1-100 nm) solid particles, is an option to achieve this target. Combining the heat exchange nature of thermosyphons and distinct thermal characteristics of nanofluids can open up new horizons in the field of heat transfer. Current study concentrates on the thermal performance of a two-phase closed thermosyphon filled with two nanofluids using water as the base fluid mixed with Al_2O_3 and $TiSiO_4$ nanoparticles. Nanofluids were prepared in different volumetric concentrations (0.01%, 0.02%, 0.05% and 0.075) and different heat loads (40W, 70W, 120W, 180W and 210W) were provided in the evaporator section. Results demonstrate that both nanofluids improve the performance through reduction in thermal resistance by 65% (at 0.05 vol.% for Al_2O_3) and 57% (at 0.075 vol.%). Other improvements were also found in the form of increase in heat transfer coefficient and decrease in evaporator wall temperature. For all the working fluids, heat transfer coefficient increases with increase in input power. Both nanofluids cause the heat transfer coefficient rise compared to that of pure water. The maximum value for heat transfer coefficient occurred at 0.05 vol.% for alumina nanoparticles, while this value took place at 0.075 vol.% for $TiSiO_4$/water nanofluid. Temperature distribution along the thermosyphon, decreased after using nanofluids as the working fluid.

Table of contents

Acknowledgements ..... **iv**

Abstrak ..... **v**

Abstract ..... **vi**

Table of content ..... **vii**

List of tables ..... **x**

List of figures ..... **xi**

List of Symbols ..... **xiv**

Chapter 1. Introduction **1**

1.1 Research background 1

1.1.1 Mechanism of thermosyphons 1

1.1.2 Characteristics of Nanofluids 2

1.2 Scope of the study 3

1.3 Significance of the study 3

1.4 Research objective 4

1.5 Organization of the study 4

Chapter 2. Literature Review **6**

2.1 Introduction 6

2.2 Heat Transfer in Heat Pipes 9

2.2.1 Constraints 9

2.2.2 Nanofluid as the working fluid: Relations 11

2.3 Nanofluid's influence on the performance: Experiments 13

2.3.1 Thermosyphons 14

2.3.2 Heat pipes 16

2.3.3 Oscillating heat pipes 20

Chapter 3. Methodology 27

3.1 Experimental setup 27

3.1.1 Thermosyphon 29

3.1.2 Joint Mount 31

3.1.3 Measuring Devices 32

3.1.3.1 Data logger 32

3.1.3.2 Thermocouples 33

3.1.3.3 Flow meter 34

3.1.3.4 Voltmeter/Ammeter 34

3.1.3.5 Pressure transmitter 35

3.1.4 Working fluids 36

3.2 Experimental procedure 38

3.3 Data reduction 40

3.4 Uncertainty Analysis 41

Chapter 4. Results and Discussion 43

4.1 Effect of nanofluids on temperature distribution 43

4.2 Effect of nanofluids on overall thermal resistance 47

4.3 Effect of nanofluids on evaporator heat transfer coefficient 50

Chapter 5. Conclusion and recommendation 57

5.1 Conclusion 57

5.2 Recommendation 58

References 60

Appendices 64

Appendix A 65

List of tables

Table 2.1. Summary of experimental studies on thermal performance of heat pipes using nanofluids 23

List of figures

Figure 1.1: Heat transfer mechanism in a thermosyphon 2

Figure 2.1: Schematic of the heat pipe model used for calculation (Shafahi, et al., 2010a)..... 11

Figure 2.2. Effect of change in concentration on the thermal resistance for concentrations of (a) 2% (b) 4% (c) 6% (d) 8%. (Alizad, et al., 2011) 12

Figure 2.3: Surface contact angle for different fluids at different temperatures (Yang & Liu, 2011)..... 15

Figure 2.4: Effect of operating pressure on the heat transfer coefficient (Liu, et al., 2007) 18

Figure 2.5. Effect of tilt angle on the heat pipe efficiency (Naphon, et al., 2009)..... 19

Figure 2.6. Change of efficiency with concentration and heat flux for the nanorefrigerant (Naphon, et al., 2009) 20

Figure 3.1. Schematic diagram of the experimental set up. 28

Figure 3.2: Image of the experimental setup..... 29

Figure 3.3: (a) Schematic of the electric circuit for the supplied power (b) Image of a band heater used in the evaporator section 30

Figure 3.4: Image of different sections of the thermosyphon without the insulation layer 31

Figure 3.5: Joint mount on top of the thermosyphon in connection with different parts 32

Figure 3.6: Images of (a) data logger (b) extension..... 33

Figure 3.7: Location of thermocouples (dimensions in cm). 34

Figure 3.8: Ammeter and voltmeter used in the experiment..... 35

Figure 3.9: Schematic of the circuit for HUBA control pressure transmitter 35

Figure 3.10: Ultrasonic homogenizer (Madell Technology Corp.)..... 37

Figure 3.11: TEM images of (a) Alumina and (b) $TiSiO_4$ nanoparticles dispersed in water at 0.05% volumetric concentration..... 37

Figure 3.12: Filling the thermosyphon with the working fluid..... 39

Figure 3.13: Vacuum pump used to achieve the negative pressure inside the pump..... 39

Figure 4.1: Repeatability of experiments for water-filled thermosyphon..... 43

Figure 4.2: Temperature distribution along the thermosyphon filled with distilled water 45

Figure 4.3: Temperature distribution along the thermosyphon filled with Al_2O_3/water nanofluid (0.05 vol.%) 45

Figure 4.4: Temperature distribution along the thermosyphon filled with $TiSiO_4$/water nanofluid (0.05 vol%) 46

Figure 4.5: Comparison of temperature distribution between water and two nanofluids for 40 W and 210 W heat loads..... 46

Figure 4.6: Operating Temperature difference Vs. input power (Al_2O_3/water nanofluid) 49

Figure 4.7: Operating Temperature difference Vs. input power ($TiSiO_4$/water nanofluid) 49

Figure 4.8: Overall thermal resistance of thermosyphon at different input powers for different concentrations of (a) Al_2O_3 and (b) $TiSiO_4$ nanoparticles..... 50

Figure 4.9: Evaporation heat transfer coefficient with respect to input power for different concentrations (Al_2O_3/water) 52

Figure 4.10: Evaporation heat transfer coefficient with respect to input power for different concentrations ($TiSiO_4$/water).....52

Figure 4.11: FESEM images of copper substrate boiled in (a) Al_2O_3/water nanofluid (0.05% vol. concentration) (b) $TiSiO_4$/water nanofluid (0.05% vol. concentration) (c) pure water.....55

Figure A.1: Temperature distribution along the thermosyphon filled with Al_2O_3/water nanofluid (0.01 vol%)……..65

Figure A.2: Temperature distribution along the thermosyphon filled with Al_2O_3/water nanofluid (0.02 vol%)……..65

Figure A.3: Temperature distribution along the thermosyphon filled with Al_2O_3/water nanofluid (0.075 vol%)……66

Figure A.4: Temperature distribution along the thermosyphon filled with $TiSiO_4$/water nanofluid (0.01 vol%)……..66

Figure A.5: Temperature distribution along the thermosyphon filled with $TiSiO_4$/water nanofluid (0.02 vol%)……..67

Figure A.6: Temperature distribution along the thermosyphon filled with $TiSiO_4$/water nanofluid (0.075 vol%)……67

List of Symbols

A_e area of evaporator (m)

Ar Archimedes number, $\frac{g \times \rho \times l^3}{\mu^2}\left(\rho_s - \rho_f\right)$

Bo Bond number, $D\left[g\frac{\rho_l - \rho_v}{\sigma}\right]^{1/2}$

Co Condensation number, $\frac{h}{k}\left[\frac{\mu^2}{g\rho^2}\right]^{1/3}$

c_p specific heat (J/kg K)

d_i inner diameter (m)

d_o outer diameter (m)

Fr Froude number, $\frac{q^2}{\rho_v D^5 h_{fg}^2 g}$

g Gravity acceleration, m/s^2

Gr Grashof number, $\frac{l^3\rho^2\beta\Delta T C_p}{\mu^2}$

h_e evaporation heat transfer coefficient (W/m^2 K)

h_{fg} heat of vaporization (kJ/kg)

I current (A)

Ja Jacob number, $\frac{h_{fg}}{C_{p,l}T_v}$

k_l liquid thermal conductivity (W/m K)

K_q Dimensionless heat transfer rate, $\frac{kl_{eva}\Delta T}{q}$

Ku Kutateladze number

k_{wall} thermal conductivity of pipe wall (W/m K)

L_e length of evaporator section (m)

M Merit number

$\dot{m}$ coolant water mass flow rate (kg/s)

m_p nanoparticle mass (kg)

Nu Nusselt number, $\frac{hD}{k}$

P input power (W)

p Pressure (Pa)

Pr Prandtl number, $\frac{\mu_l C_{p,l}}{k_l}$

Q_{out} outlet heat (W)

R_e boiling thermal resistance in evaporator (°C /W)

R_{th} Overall thermal resistance of thermosyphon (°C/W)

R_{we} Thermal resistance of evaporator wall (°C /W)

T_a adiabatic temperature (°C)

T_c condenser temperature (°C)

T_e evaporator temperature (°C)

T_{wi} inlet temperature of cooling water (°C)

T_{wo} outlet temperature of cooling water (°C)

V voltage (V)

V_p volume of nanoparticles (m^3)

V_t total volume of suspension(m^3)

Greek Symbols

σ Surface tension (N/m)

ϕ volume fraction of nanoparticles

μ_l viscosity of liquid (N s/m^2)

ρ Density (kg/m^3)

Chapter 1. Introduction

1.1 Research background

In most thermal engineering fields such as cooling of electronics and heat recovery, engineers have been trying to find ways to enhance the heat transfer mechanism. This leads to the increase in thermal efficiency, reduction in size and consequently economic feasibility. Various ways have been suggested by designers to achieve this goal among which a few have been implemented in industrial scale. The heat pipe is a device with a very high thermal conductance. The initial idea of this device was suggested by Gaugler in 1942 (Reay and Kew ,2006). However the independent invention of this device took place by Grover et al. (1964) and the significant properties of the heat pipe became appreciated. Thermosyphon, a special category of heat pipe, has been used in many different applications. Due to passive cooling capability of thermosyphons, they have been widely used in different heat transfer related applications. Due to the phase change mechanism inside these devices, a substantial increase in thermal conductivity is observed. This fact has made two-phase closed thermosyphon a common apparatus in a variety of thermal engineering areas. If changes are exerted on the design of heat pipes, the performance of this device and as a result the function of the whole system is modified. One of the options is to change the working fluid inside the pipe. Using a fluid with higher thermal conductivity compared to regular working fluids can be new solution to the problem of optimization of heat pipe performance. Nanofluids, as a new category of coolants, could be considered as one of the new candidates.

1.1.1 Mechanism of thermosyphons

In order to manufacture a thermosyphon, a small quantity of water is placed in a pipe from which the air is vacuumed and the pipe is sealed. The pipe is heated at the lower

end causing the fluid to evaporate and the vapor rises to the cold end of the pipe where it gets condensed. The condensate then returns to the hot end by the help of gravity (Figure 1.1). Due to the large latent heat of evaporation, substantial amount of heat can be transferred along with minor temperature difference from bottom to top. This implies a high thermal conductance for the device. For the two-phase closed thermosyphons, the evaporator must be situated at the lowest point in order for the condensate to return by gravitational force. However, this is considered as a limitation for this particular type of heat pipe.

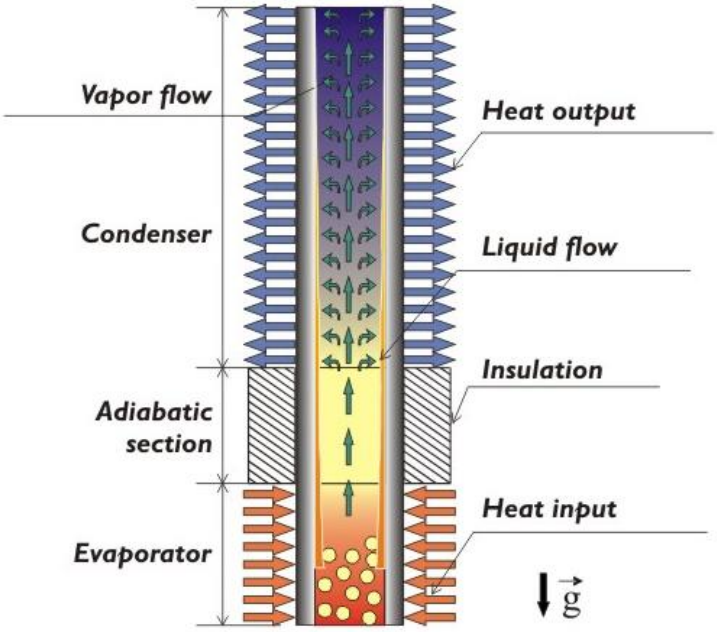

Figure 1.1: Heat transfer mechanism in a thermosyphon

1.1.2 Characteristics of Nanofluids

Since the introduction of nanofluids by Choi and Eastman (1995) , new horizons have been explored in the field of energy management. These fluids are referred to as colloids with nano-sized (less than 100 nm in diameter) particles suspended within. Water or organic liquids can be used as basefluid and solid particles can be made from

metallic or non-metallic elements, to name a few Al_2O_3, TiO_2, Cu, Au and SiO_2. Thermal behavior of these fluids has been subject of study for lots of researches. Majority of studies has outlined that existence of ultra-fine particles lead to the increase in heat transfer capability of the base fluid through enhancement in thermal conductivity. This fact has made thermal engineers consider the utilization of nanofluids in various applications. Effect of nanofluids on different heat transfer mechanisms (pool boiling, flow boiling, convection and radiation) is among the hottest research topics nowadays. The underlying reason for the special behavior shown by nanofluids is one of the most argumentative areas in which thermophoresis and Brownian motion have been indicated to be responsible. However, many parameters such as volume fraction of nanoparticles, particle size and shape are also influential on the function of nanofluids. It seems that by more investigation on the application of these new coolants, heat transfer engineering and thermal industry would be revolutionized.

1.2 Scope of the study

This study concentrates on the performance of a two-phase closed thermosyphon filled with Al_2O_3/water and $TiSiO_4$/water nanofluids. Experiments are conducted to compare the thermal performance with the case where distilled water is used as the working fluid. Important heat transfer parameters such as temperature distribution, overall thermal resistance and evaporator heat transfer coefficient will be obtained. Microscopic images from the surface will be used to explore the difference between boiling in pure water and boiling in the two nanofluids.

1.3 Significance of the study

There are a number of studies reporting the application of nanofluids in thermosyphons, but contradicting results are available on the use of Al_2O_3 nanoparticles in this application. Some studies report the enhancement while others indicate the deterioration

in the performance. The present study will hopefully shed light on the influence of alumina nanoparticles on the performance of the wickless heat pipe. Besides, for the first time, a "bimetallic" nanoparticle ($TiSiO_4$), will be implemented in a closed thermosyphon. Therefore this research will outline a comparison between a single metal nanoparticle and a bimetallic one as a working fluid in heat pipe for the first time. The change in performance parameters due to the use of nanofluid will be found and reported. In general, heat transfer capability of a working fluid is one of the main design aspects of a thermosyphon. Results of the current research may help the engineers in the fields of electronic cooling and heat recovery to have a promising idea about more efficient designs in future.

1.4 Research objectives

- To investigate the effect of Al_2O_3/water and $TiSiO_4$/water nanofluids on the temperature distribution along the thermosyphon and the overall thermal resistance
- To examine the change in the evaporator heat transfer coefficient due to use of nanofluids
- To compare the effect of different nanoparticle volumetric concentrations on performance parameters of a thermosyphon

1.5 Organization of the study

The importance and mechanism of a closed thermosyphon as well as various characteristics of a nanofluid will be introduced in chapter 1. A critical review of available literature on boiling of nanofluids, and the result of using a nanofluid in a heat pipe will be presented in chapter 2. In chapter 3, the implemented method along with a description of the experimental set up and the equipment used will be explained. Preparation of nanofluids, data and uncertainty analysis will be brought also in chapter

3. Throughout chapter 4, obtained results including the effect of nanofluids on the thermal performance and different factors such as temperature distribution, overall thermal resistance and heat transfer coefficient will be indicated. Ultimately, major findings and concluding remarks will be summarized in chapter 5 along with a number of recommendations for future researches on the same area.

Chapter 2. Literature Review

2.1 Introduction

Searching for feasible ways to optimize the performance of heat transfer devices has recently become the major focus of many researchers. Improving the heat transfer in specific devices would lead to the decrease in energy consumption as well as the size of these devices. Heat pipes and thermosyphons, two heat transfer devices with similar functions, have been widely used in thermal engineering applications. Passive cooling capability of the mentioned technologies can contribute to the significant reduction in power consumption for various industrial applications. Thanks to the phase change mechanism occurring inside these devices, a substantial increase is observed in the thermal conductivity. The main difference between the two mentioned devices stems from the fact that the former uses capillary action to return the condensed vapor to the evaporator while in the latter gravity drives the vapor from condenser section. Due to satisfactory thermal performance, these devices are widely used for various applications such as electronic device cooling, aerospace, solar heating systems and heat recovery (Akbarzadeh & Wadowski, 1996; Maziuk et al., 2001; Noie-Baghban & Majideian, 2000)

To obtain a good thermal performance, care must be taken of basic components of these devices such as the working fluid, capillary structure and the container (Reay & Kew, 2006). The role of working fluid can be very substantial since it can majorly augment the thermal performance and affect the operating temperature. Therefore, selecting an optimum fluid for the device should be done considering the boiling characteristics, compatibility with wick, vapor pressure, thermal conductivity and surface tension as well. Upon the selection of a suitable working fluid, the efficiency of heat pipe or

thermosyphon would increase and their size and weight would be reduced. Introduction of nanofluids by Choi and Eastman (1995) started a new field of research among thermal engineers. These fluids containing nano-sized (1-100 nm) solid particles have demonstrated interesting behavior in terms of heat transfer enhancement. Many factors influence the heat transfer in nanofluids such as volume fraction of nanoparticles (Eastman et al., 1999), particle size (Eastman et al., 2001) and shape (Wang et al., 1999). A number of researches have also focused on the boiling mechanism in nanofluid. In an experimental study by Das et al. (2003) degradation in the boiling of water/$Al_2O_3$and consequently an increase in the heating surface temperature were indicated. The reason was mentioned to be the entrapment of nanoparticles in the uneven surfaces, making the heating surface smoother. When concentration augmented, the wall superheat also increased implying a limit when designing cooling devices using nanofluids. Bang and Chang (2005) also reported deterioration of boiling by nanofluids due to the fouling effect caused by particle deposition that changes the surface roughness. They also mentioned a 35% enhancement in Critical Heat Flux (CHF) for horizontal flat surface. A 20% reduction in the boiling heat transfer was expressed by Jackson (2007) as well while CHF increased by about 2.8 time. You et al. (2003) varied the concentration of water/Al_2O_3 from 0 to 0.5 g/l to investigate the effect of nanoparticles on CHF where they stated an increase of 200%. Many papers have reported enhancements in boiling heat transfer of nanofluids. Buongiorno et al. (2007) studied the pool boiling behavior of Al_2O_3 and SiO_2 with water nanofluids for which they reported an increase of 68% and 56% in CHF respectively. They declared a higher nucleate boiling heat transfer coefficient for both nanofluids. Having investigated the pool boiling effects of nanofluids, Coursey and Kim (2008) found augmentations of up to 37% for different surfaces. Shi et al. (2007) investigated the effect of water based nanofluids with Fe and Al_2O_3 as nanoparticles. Their results showed that nanoparticles

enhance the boiling heat transfer due to larger thermal conductivity and having volumetric density.

The behavior of nanofluids during boiling has been closely investigated by numerous researchers to see the changes that nanoparticles exert on the phase change process of colloidal fluids. The cooling effect in heat pipes is mainly due to the phase change of working fluid. Hence, knowing the characteristics of nanofluid during boiling is essential to elucidate the performance of heat pipes under different conditions. Kim et al. (2007) observed the CHF enhancement for three different nanofluids and linked it with deposition of nanoparticles on the heating surface leading to formation of a porous layer. Improvement of surface wettability was stated to be the result of this layer and consequently a reduction in fluid contact angle which in turn augments the CHF. Same reasons were outlined in the study by Coursey and Kim (2008) as the cause of CHF enhancement. The role of nanoparticles during pool boiling of Al_2O_3/water nanofluid was experimentally identified by Wen (2012). The author mentioned the coexistence of two mechanisms to be the result of suspension of ultra-fine particles: surface modification through deposition as mentioned in previous studies plus the fact that these particles alter the bubble dynamics through changing the bubble departure volume as well as decreasing the departure frequency. The particle shape also has been indicated to be ruling as in the research by Park and Jung (2007) for carbon nanotubes (CNT), the enhancement was observed solely for low heat fluxes. The reason was noted to be that due to the shape of CNT at higher fluxes, where bubble generation is vigorous, less chance exists for particles to touch and penetrate the thermal boundary layer.

Heat pipes own a broad range of applications for heat transfer purposes. Replacing the regular fluid in this device to obtain a more efficient thermal transport might be quite a challenge. Flow of nanofluids through porous structures is still an immature concept among researchers. Existence of nanoparticles may engender some limitation in the

passive cooling ability of heat pipes. Numerous studies have been performed in this area to obtain an optimum condition for using heat pipes in terms of volume concentration, temperature range, heat flux and even the inclination of the heat pipe set up in different experimental and theoretical studies.

2.2 Heat Transfer in Heat Pipes

To clarify the heat transfer mechanism in heat pipes a number of mathematical models has been elaborated in the available literature. Some authors also have developed models for the case of using nanofluid as the working fluid in a heat pipe. In this section some of the modeling literature for regular heat pipes as well as suggested relations for heat pipes operated with nanofluids will be presented.

2.2.1 Constraints

When benefitting from the passive cooling ability of heat pipes, one faces a few constraints stemming from wick structure, fluid, operating temperature and the heat pipe length. Therefore, when modeling heat transfer and designing a heat pipe these limitations must be taken into account. One of the main concerns in the heat pipe operation is the pressure difference in two phases. To prevent the wick from drying out and to observe a correct operation from the heat pipe, a capillary limit should be taken into account for the heat flux according to equation (2.1) :

$$\Delta p_{c,\max} \geq \Delta p_l + \Delta p_v + \Delta p_g \qquad (2.1)$$

This equation implies that the maximum amount for the capillary pumping pressure must exceed the summation of all the pressure drops for the liquid (Δp_l), vapor (Δp_v) and the drop due to the gravitational head (Δp_g).

To shed more light on the mentioned limitations Nemec et al. (2013) performed calculations for different conditions for a wick heat pipe. Their computations were

based upon the correlations for various limitations such as: maximum heat fluxes due to capillary limitation, viscous limitation, sonic limitation and entrainment limit.

The equations were solved for ethanol as the working fluid. Among the constraints, boiling, entrainment and capillary were mentioned as ruling factors that should be taken care of when designing a wick heat pipe.

Regarding the capillary limit, Suman et al. (2005) also modeled the flow and heat transfer for micro heat pipes. Rectangular and triangular heat pipes were put under experiment to find the effect of apex angle on the performance. It was discovered that triangular heat pipe perform better due to smaller apex angle. Capillary pumping capacity was also said to increase for smaller dry-out lengths for the heat pipe. From the experiment done on a flat plate heat pipe, Wang and Vafai (2000) noticed facts about the performance of this type of heat pipe such as: shorter start-up time for higher input power, constant heat transfer coefficient throughout the condenser section, small variations in temperature for the outside surface of the evaporator, necessary temperature reduction in the wick to improve the performance. Using the obtained data, the authors presented correlations for maximum temperature rise $\theta_{\max}$, and difference $\Delta T_{\max}$ as well as the time constant t_c (defined as the required time for the outside evaporator surface temperature rise to get to 63.2% of its maximum value) in terms of input heat flux P:

$$\theta_{\max} = 0.376 + 0.0133P \tag{2.2}$$

$$\Delta T_{\max} = 0.289 + 8.4\times10^{-4} P \tag{2.3}$$

$$t_c = 91.4 - 0.0339P + 8.33\times10^{-6} P^2 \tag{2.4}$$

2.2.2 Nanofluid as the working fluid: Relations

Recently, with the emergence of nanofluids as cooling working fluids, some researchers have modeled heat pipes charged with nanofluids. In an analytical work by Shafahi et al. (2010a) the use of three nanofluids in a cylindrical heat pipe was modeled. The thermal conductivity model for nanofluids by Yu and Choi (2003) was implemented to take the presence of particles into account. Temperature distribution in the heat pipe was obtained for a geometry shown in Figure 2.1. The temperature distribution is used to calculate the heat transfer in the condenser region.

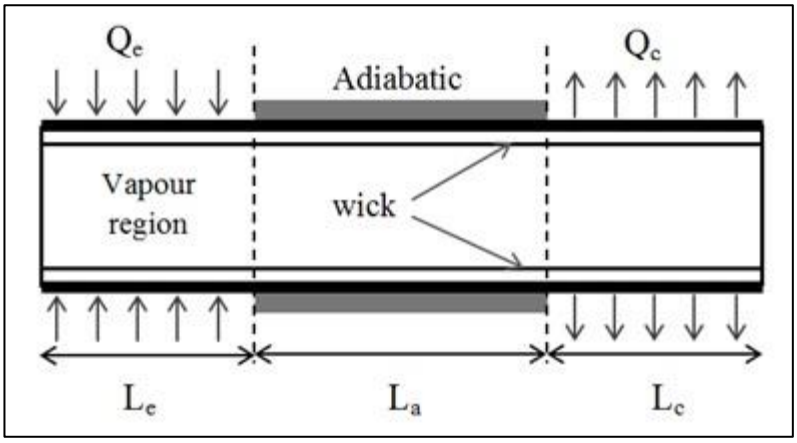

Figure 2.1: Schematic of the heat pipe model used for calculation (Shafahi, et al., 2010a)

The effects of using nanofluids were analyzed on the size reduction for the heat pipe. It was interestingly discovered that up to 78% reduction in length is achievable thanks to the use of nanofluid. Another merit of using nanofluid was reported to be the possibility of applying the heat pipe for larger heat loads (26% more heat dissipation). Using the same approach, Shafahi et al. (2010b) investigated the influence of nanofluid on the performance of a disk type and rectangular flat heat pipes. Similar enhancements were found for this type of heat pipe as well. Reduction in the temperature difference by the increase in volume concentration occurred for this study. Thermal resistance decreased about 83% and the possibility of reduction in size of the heat pipe was also resulted. For the same value of heat removal, a reduction of 30% and 20% were achievable for disk

and rectangular heat pipes. Aside from steady state analytical approach, Alizad et al. (2011) performed a transient analysis to see the effect of nanofluid on the performance of the same types of heat pipe during start-up before reaching a steady state. It was observed that a 4 s reduction takes place in the required time for the thermal layer to arrive at liquid-vapor interface. Other influences of using nanoparticles in the fluid included reduction of the size and thermal conductivity of the heat pipes used in this analytical investigation. Figure 2.2 displays the effect of particles on the thermal conductivity of the heat pipe which is generally defined as:

$$\left[P/(T_e - T_c)\right]^{-1} \tag{2.5}$$

From this figure, it can be inferred that increasing the concentration of nanoparticles causes the thermal resistance of the heat pipe to drop. This, in turn, will engender a reduction in the difference between the temperatures of condenser and evaporator.

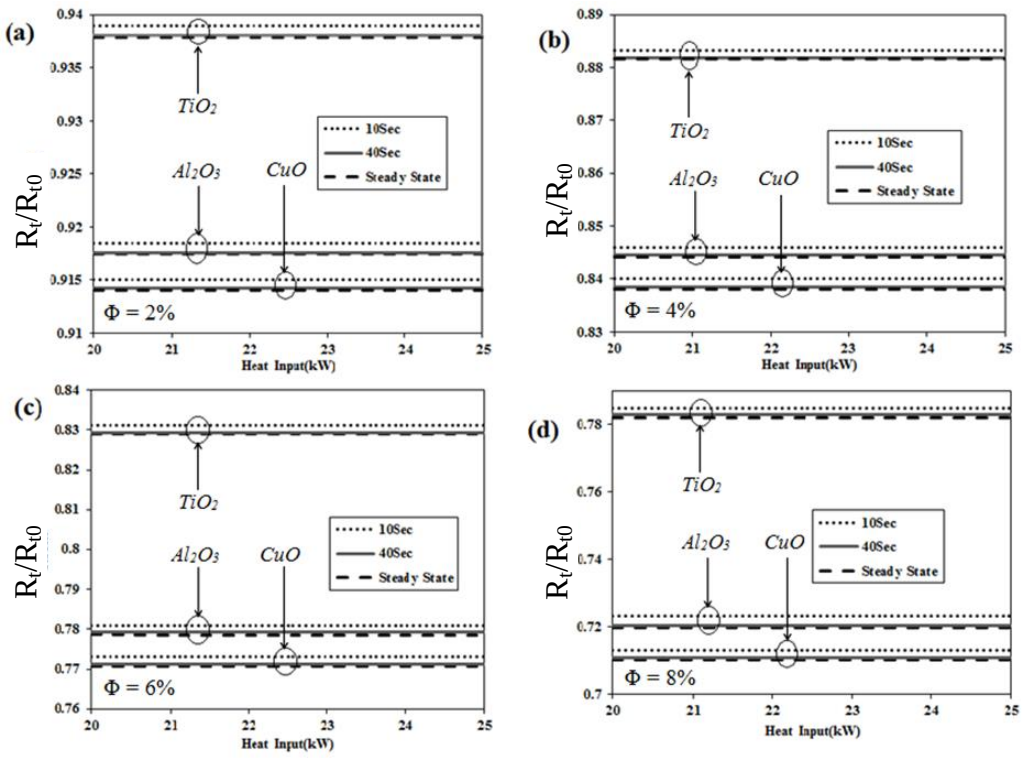

Figure 2.2. Effect of change in concentration on the thermal resistance for concentrations of (a) 2% (b) 4% (c) 6% (d) 8%. (Alizad, et al., 2011)

The study by Parametthanuwat et al. (2010) also deduced a correlation for the heat flux in a thermosyphon heat pipe using silver/water nanofluid. They indicated the Kutateladze number (*Ku)* in terms of different dimensionless parameters as in equation (2.6). This number is the criteria of maximum heat flux a thermosyphon can dissipate. As the value of *Ku* increases, there will be an augmentation in the heat flux for the device. This remained true for the case of silver/water nanofluid in the performed study. The predicted heat flux was then expressed in terms of *Ku* as in equation (2.7):

$$Ku = 3.11\left[\frac{L_e^{2.1}}{d_i}\frac{\mathrm{Pr}^{2.2}\,Bo^{2.5}Ja^{2.1}We^{1.4}Fr^{1.4}Co^{2.5}Nu^{2.5}}{Ar^{0.5}Gr^{0.5}}\right]^{0.13} \tag{2.6}$$

$$q = Ku \times \left[\rho_v h_{fg}\left(\frac{\rho_l - \rho_v}{\rho_v^2}\right)\right]^{1/4} \tag{2.7}$$

By looking at the exhibited results from the analytical/modeling studies on the application of nanofluids for passive cooling purposes, it is clear that there would be an improvement in the performance. However, the majority of the research in this area is allocated to experimental study of nanofluid behavior in heat pipes. Hence further analytical study and modeling seems to be essential to provide a broad source of data including the use of nanofluids in heat pipes.

2.3 Nanofluid's influence on the performance: Experiments

Due to the interesting characteristics of nanofluids in terms of heat transfer, a number of studies have been initiated on the use of these fluids for cooling purposes in heat pipes or thermosyphons. In most of these studies the effect of volume concentration of particles, heat flux and the tilt angle of the device set up were investigated to shed light on the functionality of nanofluids. Normally, the efficiency of a heat pipe or thermosyphon is expressed as the ratio of the heat output in the condenser to the heat input to the working fluid in the evaporator. Obviously, changing the heat transfer rates

using new working fluids would have impacts on the thermal efficiency. However, to see the relative effects on this ratio a number of experimental studies have been done that are thoroughly revised in the coming sections.

2.3.1 Thermosyphons

As mentioned before, the thermodynamics of thermosyphon is similar to that of heat pipe except for the mechanism for return of the condensate that is the gravity in lieu of capillary forces. Therefore the evaporator section must always be situated at the lowest point. Due to the absence of a wick structure, wicking limit is not considered for thermosyphons. However, a fluid must be selected to minimize the temperature drop in the device. Entrainment limit is of importance for the case of thermosyphons since if it is exceeded, condenser will be flooded. Combining the high thermal transport ability of thermosyphons and the satisfactory capability of nanofluids to transfer the heat has been recently investigated by many researchers.

Replacing the working fluid of a thermosyphon with water-based carbon nanotube (CNT) suspension, Liu et al. (2010) also measured the change in heat transfer coefficient, CHT and thermal resistance. The maximum possible input power shifted from 200 W for pure water to a value of 465 W for the CNT suspension. The heat pipe experienced a two-fold increase in the heat transfer coefficient in 2.0 vol%. A different result stemmed from using CNTs in a closed thermosyphon by Xue et al. (2006). Particles caused deterioration in the performance of the thermosyphon. Evaporation temperature and thermal resistance augmented (8°C higher and 3.3 times bigger respectively). The authors mentioned that the wettability was increased as well as the surface tension. Shin et al. (2011) conducted an experiment to compare the performances of a thermosyphon and a grooved heat pipe operating with TiO_2/water nanofluid. A reduction of 30% happened in the thermal resistance for both devices.

However, the thermosyphon owned a better performance at lower inclinations. Diameter of the thermosyphon also showed some effects on the heat transfer performance in the study by Paramatthanuwat et al. (2010) where the heat transfer rate increased in larger diameters.

Replacing the working fluid by alumina nanofluid, Noie et al. (2009) measured the improvement in heat transfer of a closed thermosyphon. Functionalizing the surface of nanoparticles by grafting silane, Yang and Liu (2011) changed the working fluid of a thermosyphon. Interestingly, they reported that for their case great stability existed and no deposition layer were created after evaporation. They also observed the change in surface contact angle for the different fluids (Figure 2.3).

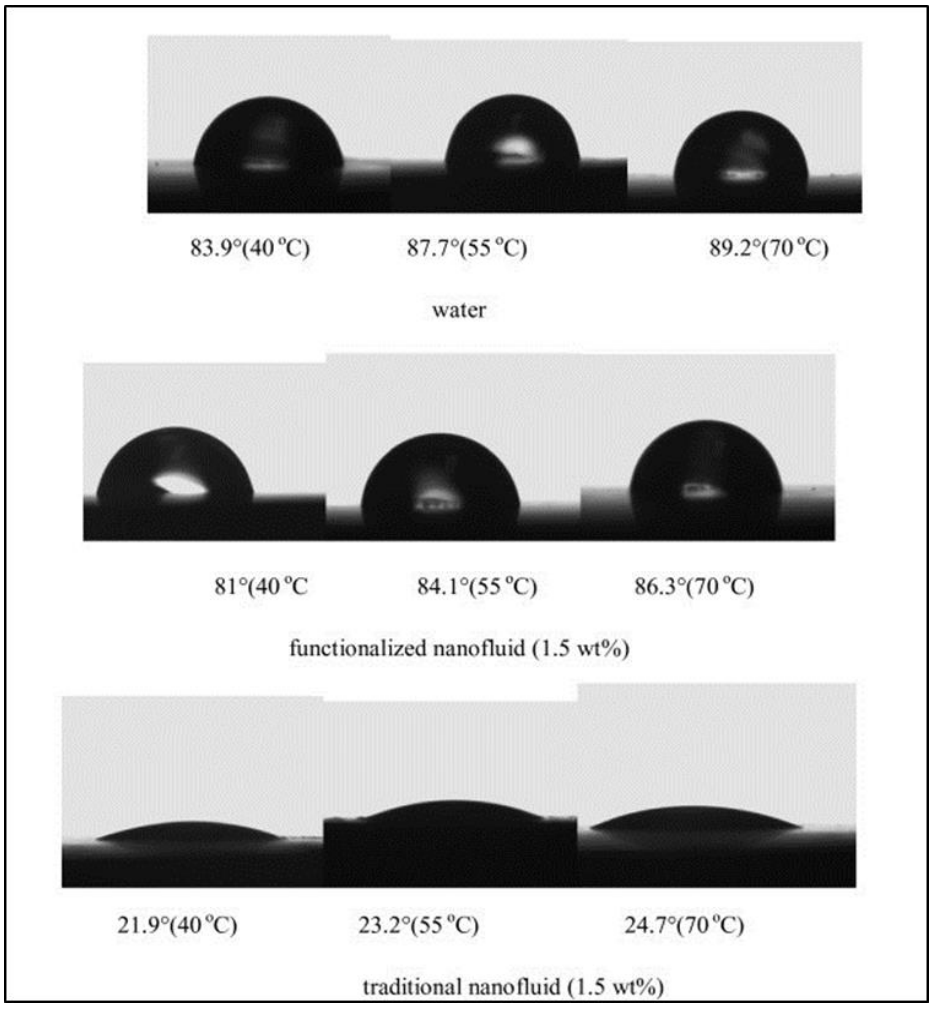

Figure 2.3: Surface contact angle for different fluids at different temperatures (Yang & Liu, 2011)

Functionalized multiwall carbon nanotubes (MWCNTs) were used in another experiment by Shanbedi et al. (2012) for a two-phase closed thermosyphon. An efficiency of 93% was found for the device in 1 wt% and heat input of 90W. A different observation is indicated in the paper by Khandekar et al. (Khandekar et al., 2008) where the performance of a thermosyphon deteriorated using Al_2O_3, CuO and laponite clay water-based nanofluids.

Aside from common nanoparticles, in the study by Huminic et al. (2011) iron oxide particles were used to investigate the thermal performance of a thermosyphon. Substantial reduction in thermal resistance was observed for this type of nanoparticles due to bombardment of created bubbles by solid nanoparticles. Other observations included 39% and 42% augmentation in the heat transfer rate for 2% and 5% volumetric concentrations for an inclination angle of 90°. Huminic and Huminic (2010) also used iron oxide nanoparticles in a thermosyphon. Impacts of inclination angle and concentration on the heat transfer mechanism of evaporator and condenser were studied. In the study, increasing the tilting angle and concentration led to augmentations in evaporation heat transfer coefficient. For the condenser, heat transfer coefficient showed an increasing trend for low operating temperatures but reduced when it came to higher temperatures. Other effects included decrease of thermal resistance via increasing the concentration (up to 5.3%) and inclination angle (30°-90°).

2.3.2 Heat pipes

Capillary forces are the key mechanism in heat pipe operation that is generated in a capillary structure constructed inside the pipe. These capillary geometries include wick structures (a porous media of felts, gauzes or sintered wicks), open grooves or covered channels. So the pressure drop through these structures become important as it can affect the performance. Flow of nanofluid in heat pipes becomes different from that in

thermosyphons since the existence of nanoparticles will affect the heat transfer and Nusselt number of the flow through the pores. This has led to some researches in this area.

Using Alumina nanofluid, Teng et al. (2010) investigated the thermal efficiency of a straight copper heat pipe. They varied the charge amount to see its effect on the thermal behavior of the pipe. They indicated that by using nanofluid, an optimum operating condition could be achieved with a rise of nearly 17% in thermal efficiency along with a reduction of 40% in fluid charge amount. In another experiment by Do et al. (2010) effect of Al_2O_3/ water nanofluid on the thermal resistance of a heat pipe with screen mesh wick was studied. The authors reported a 40% decrease in thermal resistance. Using titanium nanoparticles in alcohol, Naphon et al. (2008) found an augmentation of 10.6 % in the thermal efficiency by 0.1% volume concentration. Do and Jang (2010)solved the conduction and phase change equations for Al_2O_3/water nanofluid in a grooved wick heat pipe.

In their experiment for CuO /water nanofluid in a mesh heat pipe, Liu and Zhu (2011) found lower average wall temperature for the case of nanofluids. However, the increasing trend were not uniform for heat transfer coefficient and the maximum heat flux in terms of mass concentration (the maxima for both parameters belonged to 1.0 wt%). A circular heat pipe was subjected to a flow of aqueous gold nanoparticles by Tsai et al. (2004) and the results of changes in the thermal resistance were analyzed. A relative large reduction observed in the thermal resistance of evaporator section compared with condenser section.

Investigating the effect of alumina-water nanofluid on the operation of a circular heat pipe, Mousa (2011) indicated that a decrease in thermal resistance would occur thanks to the use of nanofluid. He also presented a correlation including the effect of dimensionless heat transfer rate (K_q), filling ratio (FR) and Prandtl number on the

thermal resistance (equation (2.8)). However, the improvement in the performance was stated to diminish when augmenting the concentration.

$$R = 0.294\left[k_q^{-0.596} FR^{1.273} \mathrm{Pr}^{-0.0532}\right] \tag{2.8}$$

Liu et al. (2007) announced another factor to be effective on the thermal performance which was the operating pressure. Their results are shown in Figure 2.4. It can be noted that there is an inverse relation between the heat transfer coefficient and the operating pressure ranging from 7.4 kPa to atmospheric pressure. The possible cause for this observation was mentioned to be the greater forming and departure of generated bubbles under sub-atmospheric pressures.

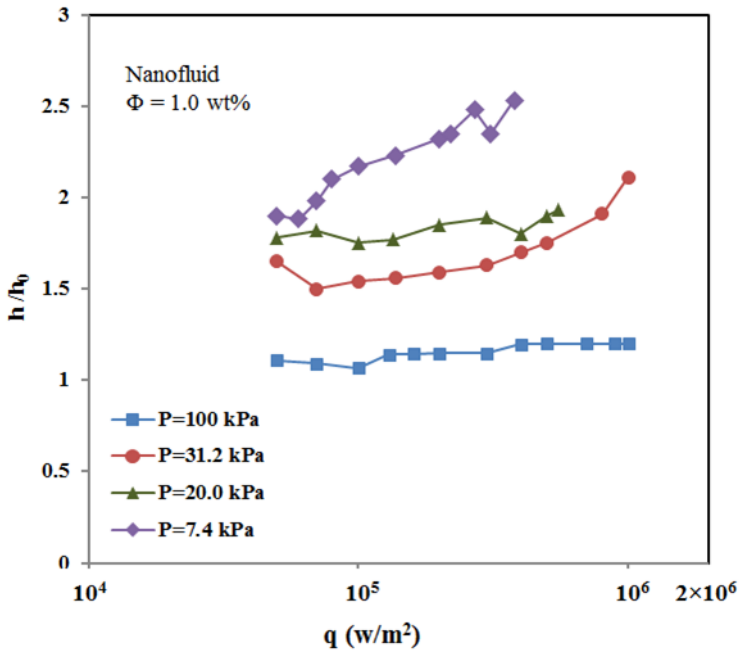

Figure 2.4: Effect of operating pressure on the heat transfer coefficient (Liu, et al., 2007)

In the experiment by Yang et al. (2008) the effect of CuO nanoparticles on the functionality of a micro-grooved heat pipe was studied. 1.0% concentration showed the optimum conditions in terms of the heat transfer. Silver nanoparticles were dispersed in water to be used in a grooved heat pipe by Kang et al. (2006). Two effects were investigated including the concentration and size of the nanoparticles. It was outlined

that particles' size would change the nanofluids role as 50% and 80% reductions in thermal resistance were achieved for particle sizes of 10 nm and 35 nm respectively. The augmentation in particle concentration also led to reduction in the generated increment of heat pipe wall temperature. Wang et al. (2010) used Cuo/water nanofluid to see its effects on the operation characteristics. Role of inclination angle on the evaporator and condenser heat transfer and effect of pressure on the amount of heat flux for a grooved heat pipe run by CuO/ was investigated experimentally by Liu et al. (2010). At the optimum angle of 75°, maximum heat transfer augmentation occurred for both sections.

Naphon et al. (2009) also tested the effect of changing the working fluid to a nanofluid. Differently, they used R11 refrigerant as the base fluid for the titanium oxide nanoparticles. Figure 2.5 and Figure 2.6 show the results including the effect of tilt angle, heat flux and concentration on the efficiency.

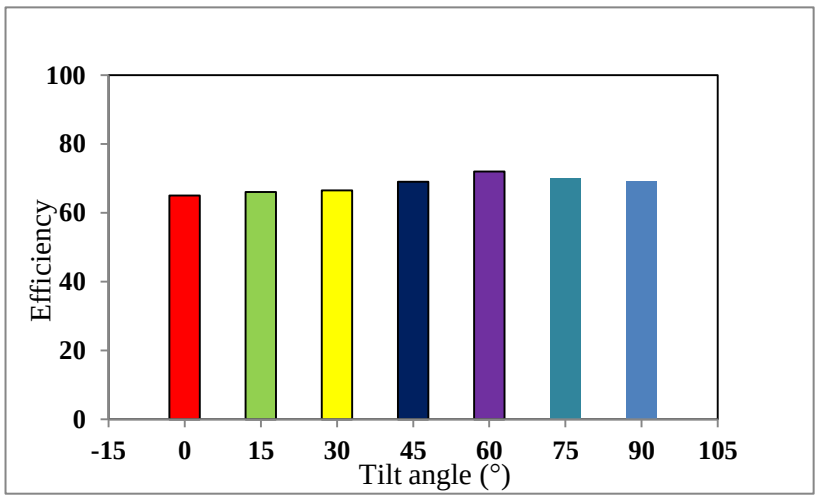

Figure 2.5. Effect of tilt angle on the heat pipe efficiency (Naphon, et al., 2009)

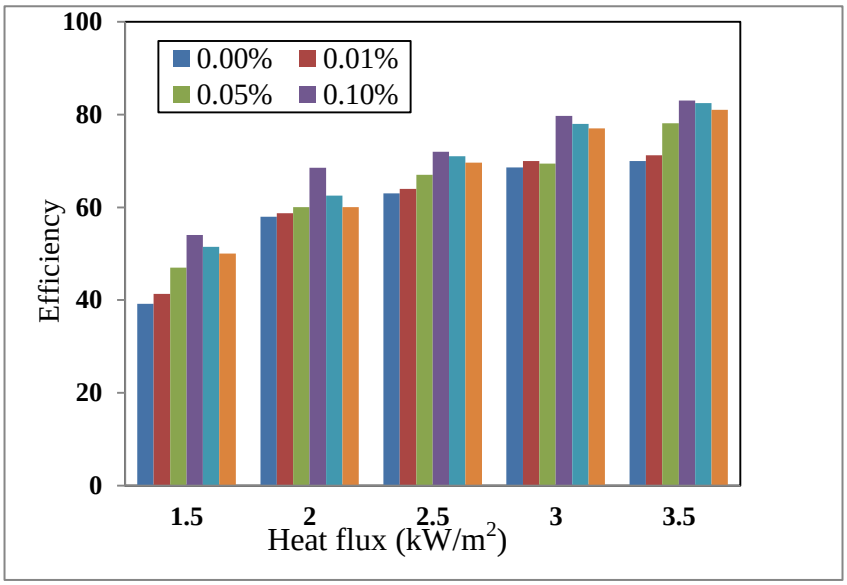

Figure 2.6. Change of efficiency with concentration and heat flux for the nanorefrigerant (Naphon, et al., 2009)

Wang et al. (2012) investigated the influence of nanofluid on a mesh wicked heat pipe performance. Three operating conditions in terms of temperature and pressure were maintained for the experiment. Thermal resistance decreased by 58% and 55% for horizontal and vertical positions respectively. Comparing the effect of three different particles (TiO_2, Al_2O_3 and ZnO) in two base fluids (water, ethylene glycol), Putra et al. (2012) tested the performance of screen mesh heat pipes. Al_2O_3/water nanofluid showed the top improvement with the lowest evaporator temperature and the highest evaporator heat transfer coefficient.

2.3.3 Oscillating heat pipes

In these types of heat pipe, working fluid is filled in the capillary dimension channel in which slugs of fluid interspersed with bubbles of vapor are generated due to surface tension. One side of the capillary tube is heated in the evaporator section that causes the bubbles to grow. Enlarged bubbles force the liquid towards the condenser section where the temperature of the flow would be reduced. This cooling will decrease the vapor pressure and causes a continuous growth and collapse of bubbles in evaporator and

condenser sections and consequently an oscillating motion would occur within the tube. Therefore, the heat coming from the source will be converted to kinetic energy of the fluid. The interesting aspect about these types of heat pipes would be the intensification of forced convection by the oscillations aside from the boiling/condensation inside the tubes.

One of the early studies was done by Ma et al. (2006) where the effect of diamond/water nanofluids was examined for an oscillating heat pipe. Unlike the pure fluid, the temperature difference between evaporator and condenser would start increasing at a certain heat flux. The oscillating nature of the flow was stated to be in charge of this observation. With a rise in the input heat flux, the pulsating motion began to grow stronger. The effective thermal conductivity of the nanofluid stopped to increase due to the oscillating motion. Consequently, the temperature difference started to increase. Silver/water nanofluid was tested in an oscillating heat pipe in another experiment by Lin et al. (2008) with changing heat flux, filling ratio as well as the particle concentration. The authors claimed that extremely high or excessively low filling ratio would hinder the bubble pulsation or heat pipe dry out respectively. Wannapakhe et al. (2009) also used silver nanoparticles water for an OHP. They found the satisfactory results in terms of heat transfer improvement. Role of alumina nanofluid in an oscillating heat pipe was compared with that of a microcapsule fluid by Wang et al. (2009). The microcapsule fluid contained phase change particles with average size of 1 μm with a melting temperature of 39.66°C. For the same conditions, both fluids were put in comparison with pure water. Two heating conditions including vertical bottom and horizontal bottom were applied to the heat pipe. For the former heating, the microcapsule fluid showed better performance while Al_2O_3/water mixture performed better in the horizontal bottom heating conditions. Reductions of 0.35°C/W and 0.19°C/W were announced for in the thermal resistance for the microcapsule fluid and

the nanofluid respectively. Nonetheless, nanofluid owned better performance for the horizontal bottom heating.

Que et al. (2010) observed the improved performance of an OHP filled with Al_2O_3 and justified the reduction in thermal resistance in a comprehensive way. In their study, total thermal resistance was comprised of four types: conductive in the wall, thermal resistance in two-phase flow and boiling/condensation resistances in evaporator and condenser. It was inferred that the major change was exerted on the resistance of the evaporator after using nanofluids.

Other statements were made by Riehl and Santos (2011) on the performance of copper/water nanofluid. They indicated that the pulsations occurred with higher amplitudes since nanoparticles enhanced the slug dynamics. Another contribution to the enhancement of thermal performance was caused by the smaller critical diameter for bubbles. Changing the shapes of nanoparticles, Yulong et al. (2011) ran an experiment with an oscillating heat pipe filled with alumina nanofluids. They observed that aside from other factors, shape is also influential on the heat transfer enhancement. The authors found that for the same conditions cylinder type particles produce the best results along with a 78% of enhancement in efficiency.

Table 2 presents a summary of the experimental studies on the application of nanofluids in heat pipes. In general previous studies show that using nanofluid can enhance the heat transfer capability of a heat pipe. This means that using nanofluids in a heat pipe efficiency of some thermal systems will be reduced while reducing the size and bulkiness of the system. In terms of application, higher heat inputs can be removed by heat pipes using nanofluids due to their high heat capacity.

Table 2.1. Summary of experimental studies on thermal performance of heat pipes using nanofluids

Reference	Type of Device	Nanofluid	Results
Liu et al. (2010)	Miniature thermosyphon	CNT/water	Particle concentration, operating pressure, heat flux affect the performance/ thermal resistance and wall temperature decrease due to nanofluid
Xue et al. (2006)	Thermosyphon	CNT/water	Nanotubes degrade the thermal performance of the device/ Thermal resistance and evaporator temperature increased
Shin et al. (2011)	Thermosyphon/grooved heat pipe	TiO_2/water	Thermosyphon works better than the heat pipe with nanofluid at lower angles/ increasing volume concentration decreases the thermal resistance
Paramatthanuwat et al. (2010)	Thermosyphon	Silver/water	Heat transfer rate and filling ratio augments for the case of nanofluid
Noie et al. (2009)	Thermosyphon	Al_2O_3/water	Efficiency improved up to 14.7% /less temperature difference occurred between evaporator and condenser
Yang and Liu (2011)	Thermosyphon	SiO_2/water (functionalized vs. normal)	Functionalized nanofluid enhances performance without changing MHF/Normal nanofluid deteriorates the evaporator heat transfer but enhances MHF
Shanbedi et al. (2012)	Thermosyphon	MWCNT/water	Thermal efficiency augments (up to 93%) by using nanofluid up to a maximal amount at an optimum heat input and concentration/ vacuum pressure drops
Khandekar et al. (2008)	Thermosyphon	Al_2O_3, CuO, laponite clay/water	Nanofluids deteriorate the thermal performance of the thermosyphon
Huminic et al. (2011)	Thermosyphon	Iron oxide/water	Heat transfer increases/ thermal resistance decreases with increasing particle concentration

Huminic and Huminic (2010)	Thermosyphon	Iron oxide/water	Nanofluid enhances the thermal efficiency/Increasing inclination angle augments the heat transfer but reduces the thermal resistance
Teng et al. (2010)	Straight cylindrical heat pipe	Al_2O_3/water	Thermal efficiency improves/fluid charge amount decreases
Do et al. (2010)	Circular screen mesh wick heat pipe	Al_2O_3/water	Both thermal resistance and evaporator wall temperature decrease/ maximum heat transfer rate enhances
Naphon et al. (2008)	Straight cylindrical heat pipe	TiO_2/ water, alcohol	Up to 11% improvement in thermal efficiency is possible/ efficiency increases by augmenting the heat flux
Do and Jang (2010)	Flat grooved heat pipe	Al_2O_3/water	Performance enhances at an optimum concentration/ thermal resistance decreases
Liu and Zhu (2011)	Straight cylindrical mesh heat pipe	CuO/water	Heat transfer coefficient increases by reducing the pressure/lower average wall temperature for the case of nanofluid
Tsai et al. (2004)	Straight cylindrical heat pipe	Gold/water	Higher thermal performance/ up to 37% reduction in thermal resistance
Mousa (2011)	Straight circular heat pipe	Al_2O_3/water	Thermal performance deteriorates with increasing the concentration
Liu et al. (2007)	Miniature flat heat pipe	CuO/water	Thermal performance improves by nanofluid but at an optimum volume concentration/operating pressure has substantial effects on the performance
Yang et al. (2008)	Micro-grooved heat pipe	CuO/water	Thermal resistance reduces/operating pressure affects the performance

Kang et al. (2006)	Grooved circular heat pipe	Silver/water	Changing the particle diameter and concentration affects the thermal resistance
Wang et al. (2010)	Miniature grooved heat pipe	CuO/water	Use of nanofluid reduces the start-up time for unsteady operation/ for steady operation evaporator heat transfer coefficient and CHF are increased
Liu et al. (2010)	Grooved heat pipe	CuO/water	Operating pressure and inclination effect the performance/ nanofluid increases the maximum heat flux
Naphon et al. (2009)	Straight cylindrical heat pipe	TiO_2/ R11	Thermal efficiency reaches a maxima at an optimum condition of concentration and tilt angle
Wang et al.(2012)	Miniature mesh heat pipe	CuO/water	Nanofluid enhances the evaporator/condenser heat transfer, reduces the thermal resistance/ inclination angle and operating temperature affect the performance
Putra et al. (2012)	Screen mesh heat pipe	TiO_2, Al_2O_3,ZnO/water, ethylene glycol	Alumina showed higher enhancement in performance compared to other two particles
Ma et al. (2006)	Oscillating heat pipe	Diamond/water	Temperature difference between evaporator and condenser decreases
Lin et al. (2008)	Oscillating heat pipe	Silver/water	Heat transfer is improved, temperature difference and thermal resistance is reduced
Wannapakhe et al. (2009)	Oscillating heat pipe	Silver/water	Performance improves by silver particles mixed with water
Wang et al. (2009)	Pulsating heat pipe	Al_2O_3/water	Thermal resistance is reduced
Qu et al. (2010)	Oscillating heat pipe	Al_2O_3/water	Evaporator thermal resistance is reduced due to change of surface conditions

Que and Wue (2011)	Oscillating heat pipe	SiO_2,Al_2O_3/water	Performance improves by alumina particles but deteriorated with silica particles
Riehl and Santos (2011)	Oscillating heat pipe	Cu/water	Thermal performance is improved/ wall temperature is lowered
Yulong et al. (2011)	Oscillating heat pipe	Al_2O_3/water, ethylene glycol	Particles with cylindrical shape induce more enhancement on thermal performance

Chapter 3. Methodology

In the following sections details about the experimental procedure and the specifications of the equipment used will be presented. Also, the preparation of nanofluids, and the uncertainty analysis will be brought in this chapter.

3.1 Experimental setup

It is important that researchers know how to perform successful tests, and it is equally important that they be wary of the accuracy of their measurements. In this section the equipment used in the experiment including measurements devices, the main test section and their corresponding accuracy will be expressed in a detailed way.

The schematic of the experimental setup is depicted in Figure 3.1. The test rig was located in the Heat Pipe Laboratory of Monash University, Sunway campus. The actual setup can be observed in Figure 3.2. The setup mainly consists of the following components:

- Two-phase closed thermosyphon comprised of evaporator, adiabatic and condenser sections
- Joint mount
- Different measuring devices
- Working fluids

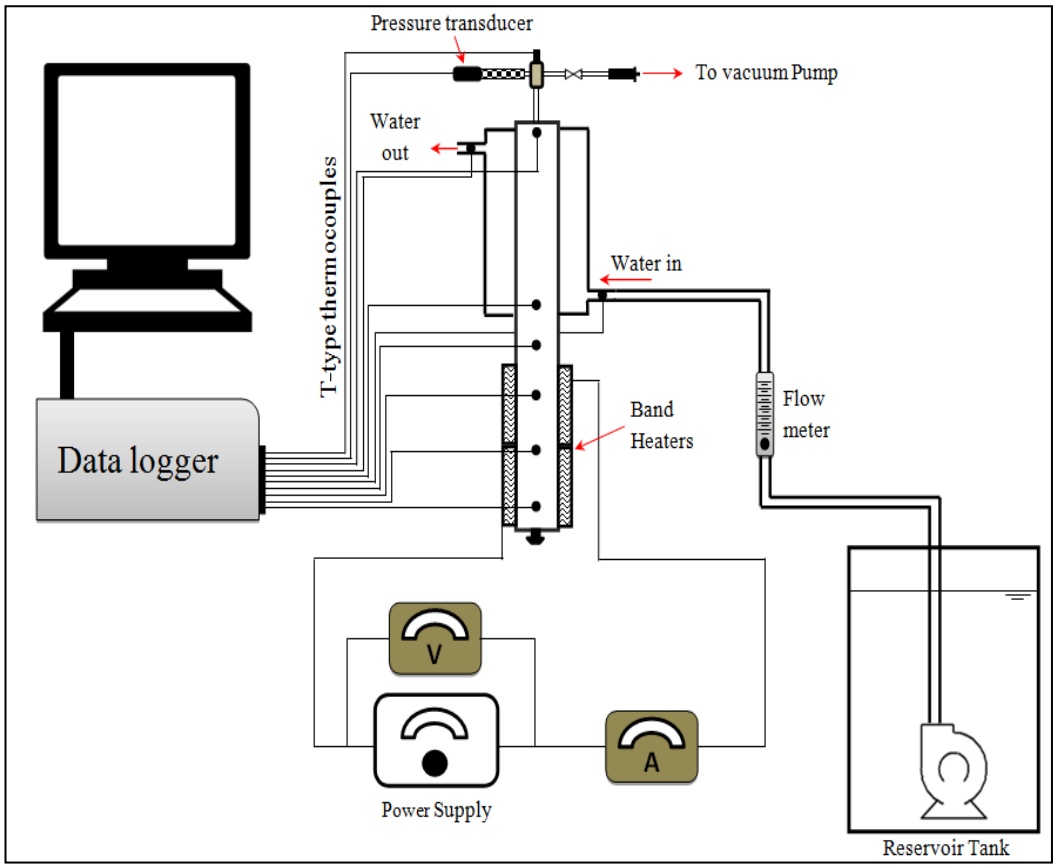

Figure 3.1. Schematic diagram of the experimental set up.

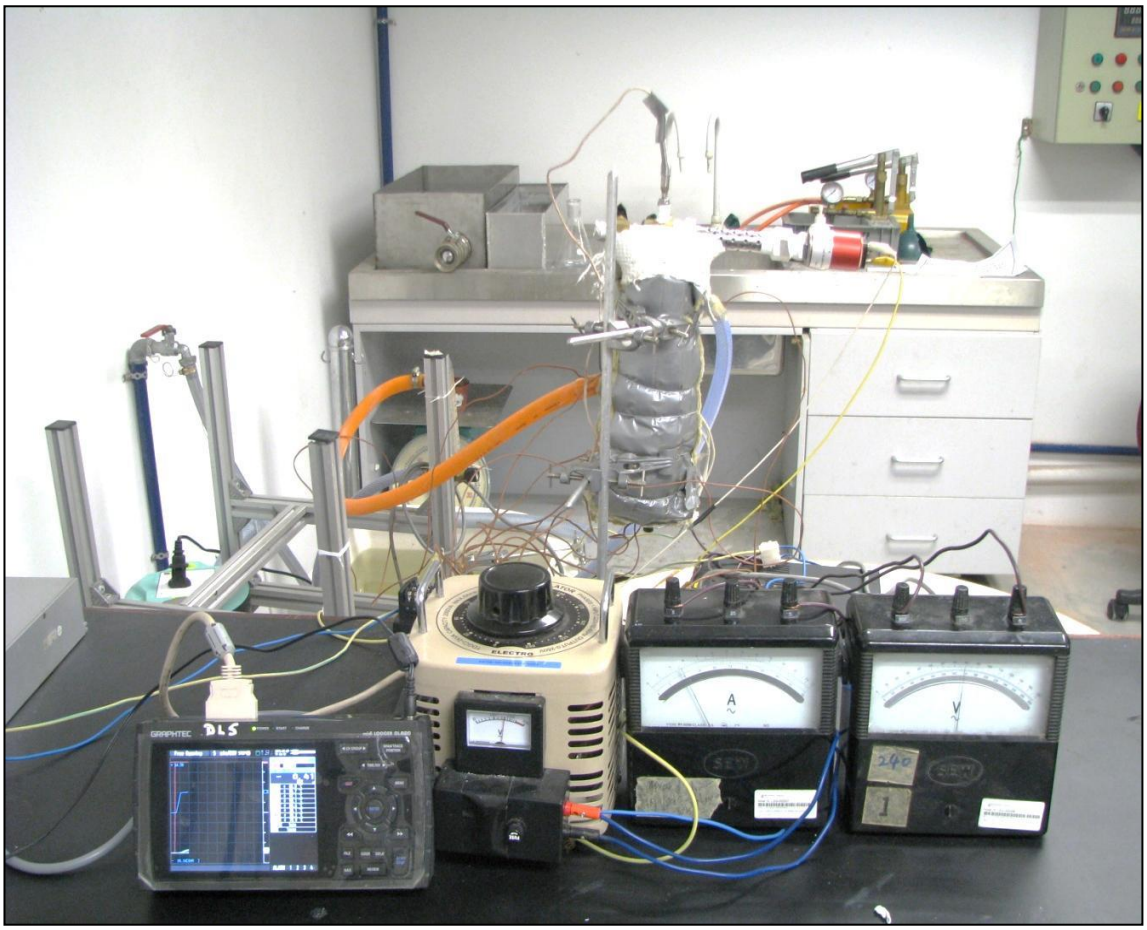

Figure 3.2: Image of the experimental setup

3.1.1 Thermosyphon

The heat pipe used in this experiment was a circular tube made of copper without any wick inside. The pipe has an inner diameter of 19 mm and a wall thickness of 1.7 mm. The length of the thermosyphon is equal to 30 cm and consists of the following sections:

- Evaporator (10 cm)
- Adiabatic (6 cm)
- Condenser (14 cm)

Evaporator section, which is subjected to heat loads, is covered with two band heaters each rated at 250Ω. The power was supplied to the heaters through establishing an electric circuit as seen in Figure 3.3.

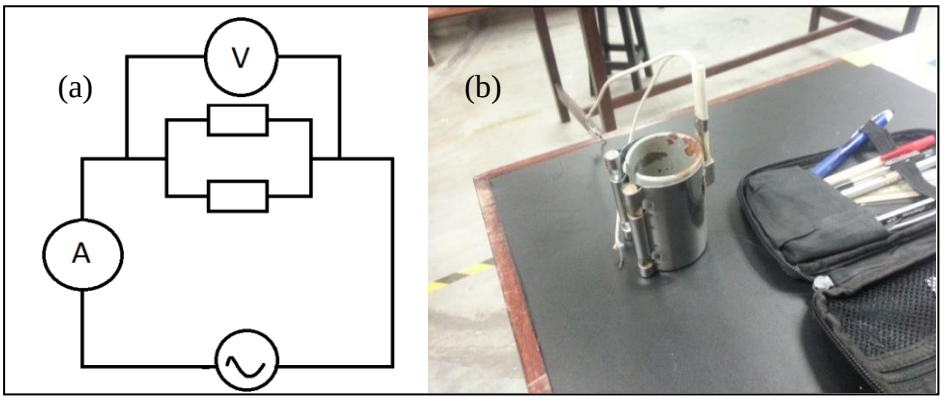

Figure 3.3: (a) Schematic of the electric circuit for the supplied power (b) Image of a band heater used in the evaporator section

The condenser section includes part of the heat pipe surrounded by a cooling jacket with an outside diameter of 55 mm. The jacket is constructed of copper and brass pieces to cover the gaps, followed by welding to the pipe body. Water inlet is located at the bottom while an outlet is put on top for water to go to drain. Cooling water was pumped from a reservoir tank to the cooling jacket. The volume flow rate was maintained as constant using a flow meter. Figure 3.4 shows the thermosyphon along with labeled different sections without insulation.

In order to ensure that heat losses from the thermosyphon are minimized, a 6 cm thickness of rock wool insulation (thermal conductivity equal to 0.045 W/m K) was installed around the pipe.

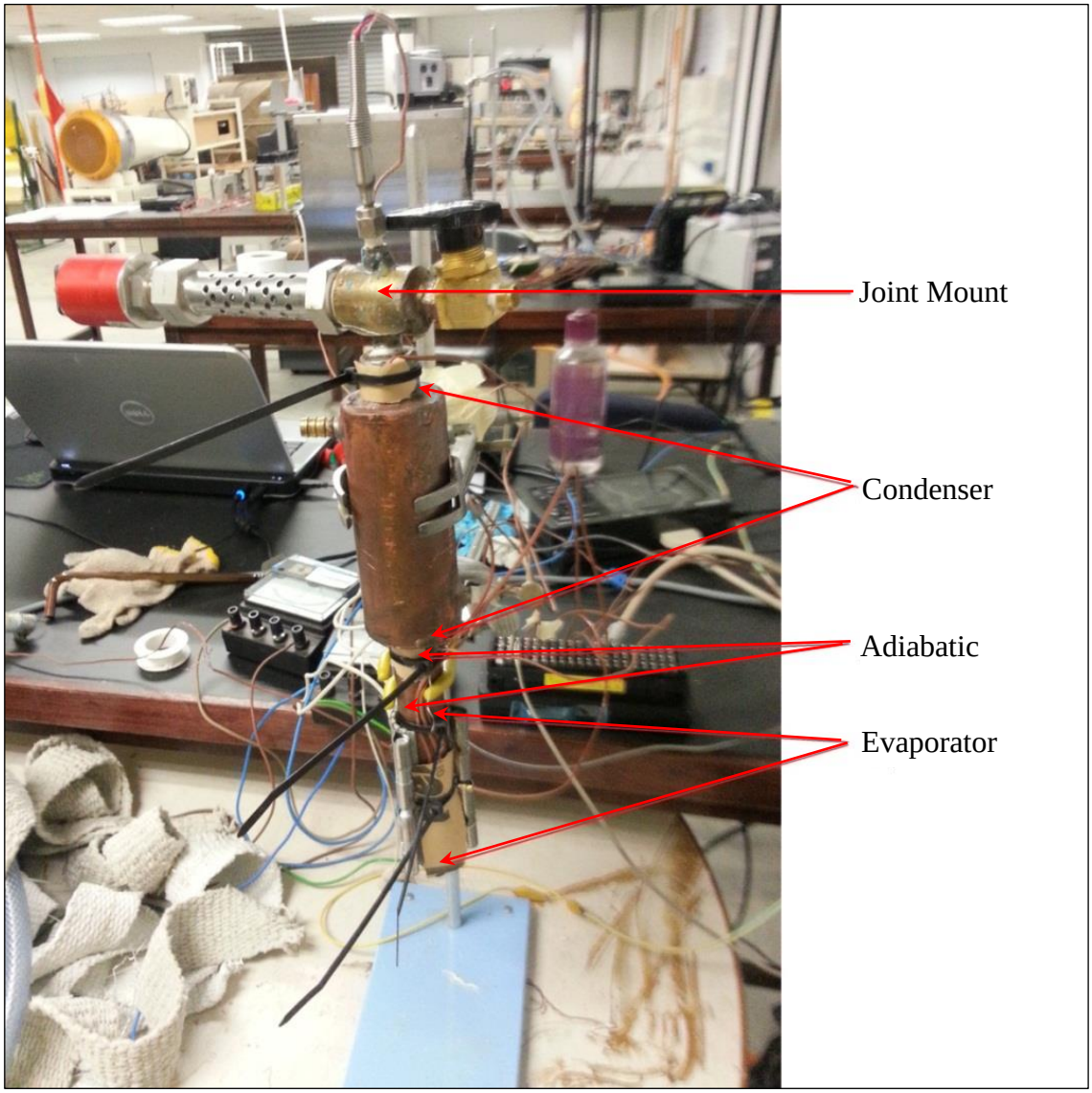

Figure 3.4: Image of different sections of the thermosyphon without the insulation layer

3.1.2 Joint Mount

In order to connect the required measuring devices and filling inlet a joint mount, made of brass, was welded on top of the thermosyphon. This joint was used to integrate the following parts into the test section (Figure 3.5):

- Vacuum valve
- Pressure transmitter
- Thermocouple

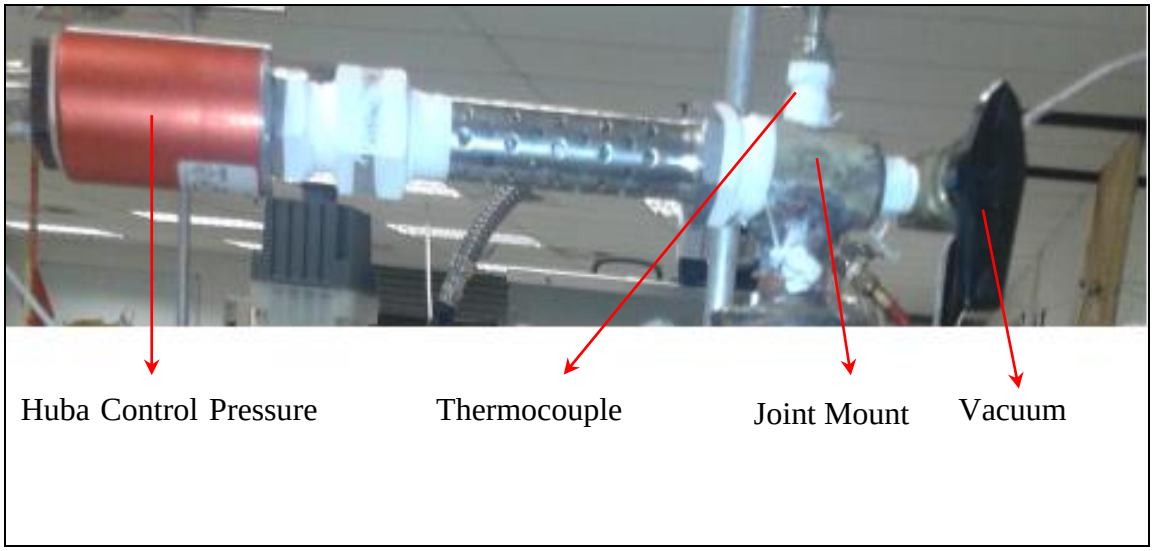

Figure 3.5: Joint mount on top of the thermosyphon in connection with different parts

3.1.3 Measuring Devices

In this section the devices used to measure the required parameters including temperature, pressure and power will be explained in detail. Thermocouples, pressure transmitter, voltmeter, ammeter and flow meter were the main measuring devices used in this experiment. The data acquisition system will also be indicated hereby.

3.1.3.1 Data logger

Graphtec GL820E Midi Data Logger was used to record the measured parameters in the experiment. A terminal extension was also used along with the logger. The data logger and the terminal are shown in Figure 3.6. This data acquisition system is proper to record voltage, temperature, humidity, pulse and logic signals. It is capable of measuring parameters such as voltage and temperature simultaneously. It is possible to expand the channels up to 200 channels. The device has also a 2 GB built-in flash memory. The voltage input can be in the range of 20 mV to 50 V and the thermocouples types that can be used with this data logger include: K, J, E, T, R, S, B, N, and W.

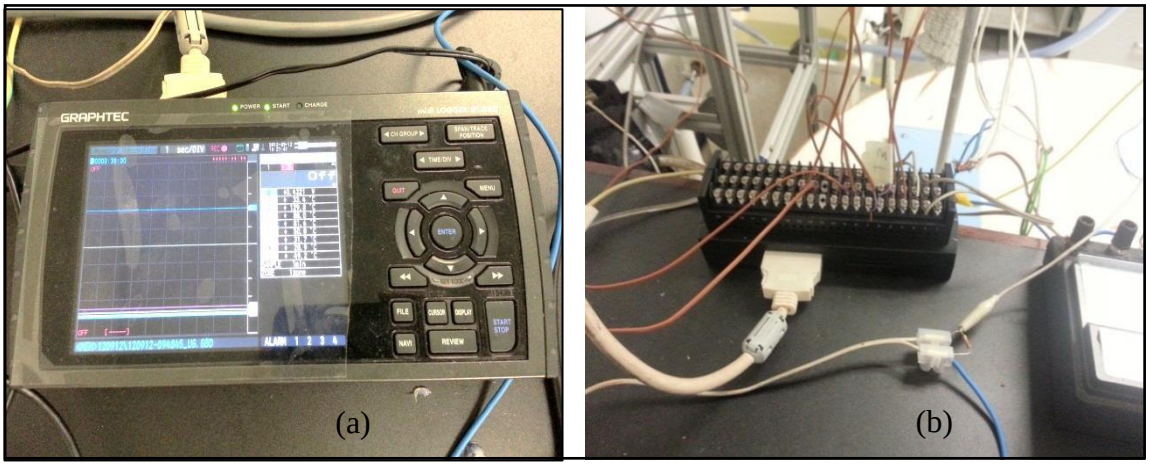

Figure 3.6: Images of (a) data logger (b) extension

3.1.3.2 Thermocouples

T-type thermocouples (bought from OMEGA ENGINEERING, INC) were used to measure the temperatures needed in the experiment. 9 thermocouples were installed on the surface of the thermosyphon among which three were placed on the evaporator (T_{e1},T_{e2} ,T_{e3}), two on adiabatic section (T_{a1},T_{a2}) and one on the upper part of the thermosyphon to give us the temperature of the condenser (T_c). These thermocouples were installed using thermal paste and a layer of anti-flame paper was used to hold them tightly to the surface. Two thermocouples were also inserted in the inlet and outlet hoses to measure the inlet and outlet water temperature (T_{wi},T_{wo}). Another probe was inserted into the pipe to measure the saturation temperature. Figure 3.7 demonstrates the location of installed thermocouples on the test section.

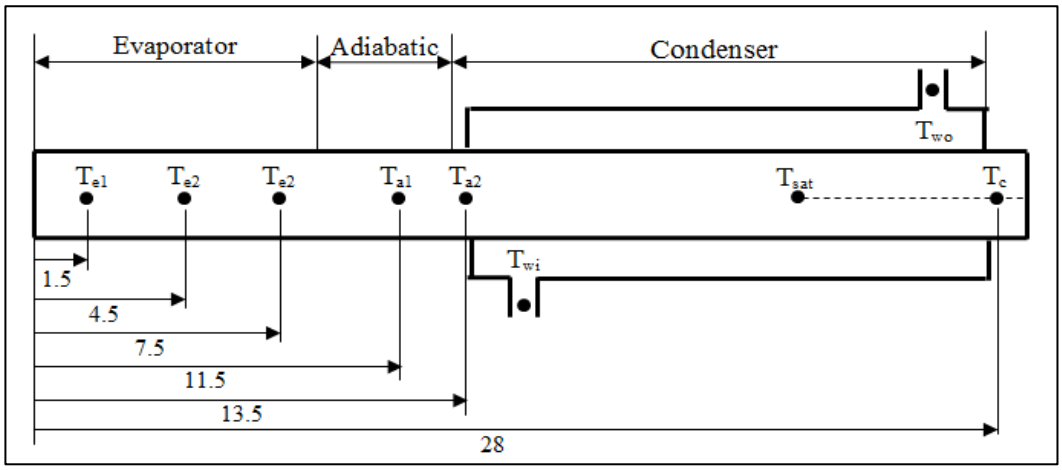

Figure 3.7: Location of thermocouples (dimensions in cm).

3.1.3.3 Flow meter

The flow meter used in the experiment measures the minimum flow rate of 2 liter per minute and a maximum flow rate of 20 liter per minute. However, for our application a flow rate of 12 ml/s was required. Therefore, the cooling water flow rate was also measures manually. The time needed for filling a 200 ml beaker was recorded and the flow rate was adjusted to achieve the desired value. Time recording was repeated 6 times to minimize the error in measuring the flow rate.

3.1.3.4 Voltmeter/Ammeter

Both voltmeter and ammeter were purchased from STANDARD ELECTRIC CO. LTD.

The ammeter comes in three different scales of 5, 10 and 25 A. The voltmeter also comes in various scales of 75, 150 and 300 V. Figure 3.8 shows the image of ammeter and voltmeter used in the test rig.

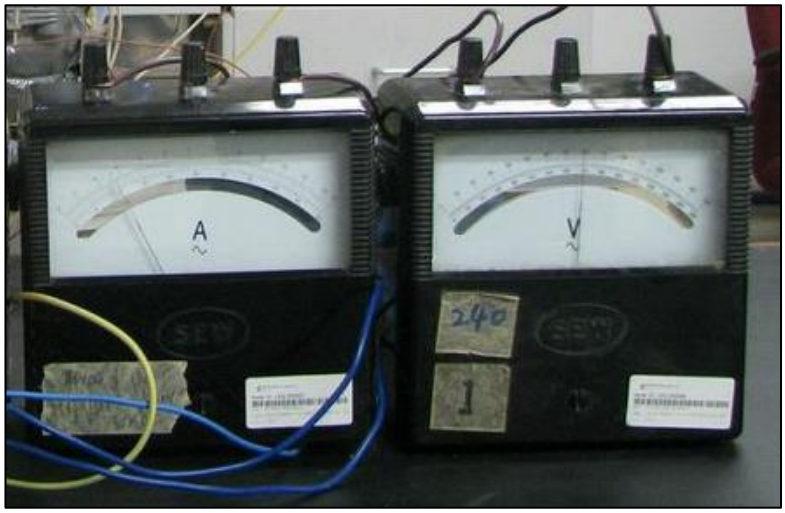

Figure 3.8: Ammeter and voltmeter used in the experiment

3.1.3.5 Pressure transmitter

Saturation pressure was measured with the aid of the pressure transmitter called HUBA control (Model 691.53300716, Switzerland). This device transmits 0.4mA-20mA through its two outputs. This is then translated into a readable voltage reading which will be converted into pressure readings afterwards. The pressure transmitter was installed into a circuit according to the instructions given by manufacturer. The schematic of the circuit is brought in Figure 3.9.

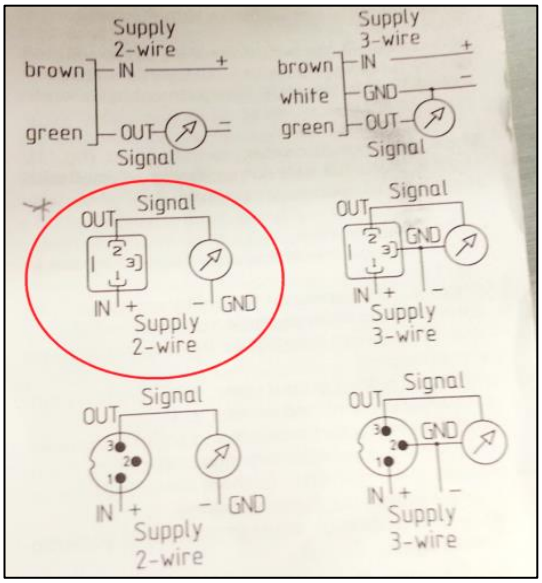

Figure 3.9: Schematic of the circuit for HUBA control pressure transmitter

3.1.4 Working fluids

Two types of nanoparticles were used in the experiments including Al_2O_3 (13 nm, 99.8% metals) and $TiSiO_4$ (<50 nm, 99.8% metals) purchased from Sigma Aldrich, Inc. A two-step method was performed to prepare the nanofluids. Particles were weighed using a high precision balance before getting mixed. These nanoparticles were dispersed in distilled water using ultrasonic homogenizer. The ultrasonic homogenizer was a digital one purchased from Madell Technology Corp. The device is shown in Figure 3.10.The sonication was maintained at sound frequency of 50 kHz to attain a uniform and stable dispersion of particles. In order to avoid any possible changes in the properties of nanofluids, no surfactants were used in this study. Nanofluids were prepared in volume fractions of 0.01%, 0.02%, 0.05% and 0.075%. These samples were prepared according to the following expression of volume fraction and density of nanoparticles:

$$\phi = \frac{V_p}{V_t} \tag{3.1}$$

$$\rho_p = \frac{m_p}{V_p} \tag{3.2}$$

Therefore, to prepare 1 liter of nanofluid, the following amount of nanoparticles would be required:

$$m_P = 1\times10^3 \phi.\rho_p \tag{3.3}$$

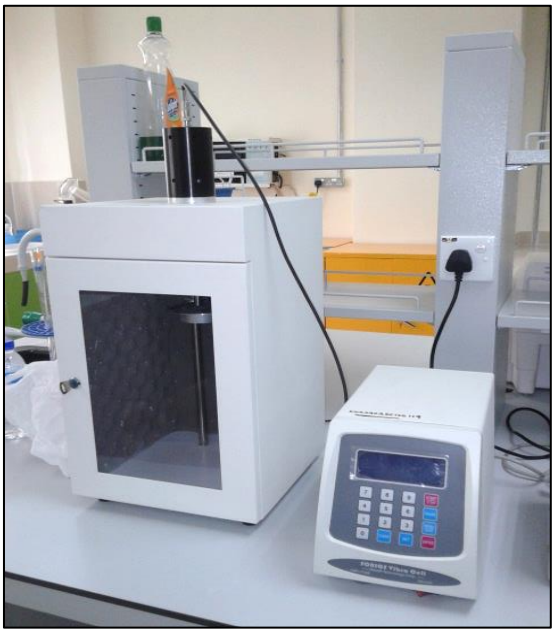

Figure 3.10: Ultrasonic homogenizer (Madell Technology Corp.)

Figure 3.11 shows the Transmission Electron Microscopy (TEM) images of Al_2O_3 and $TiSiO_4$ nanoparticles at 0.05 vol.%. The spherical shape of $TiSiO_4$ nanoparticles can be distinctly seen in the figure. After sonication, the nanofluids were put under observation and no sedimentation occurred after 48 h of being kept static.

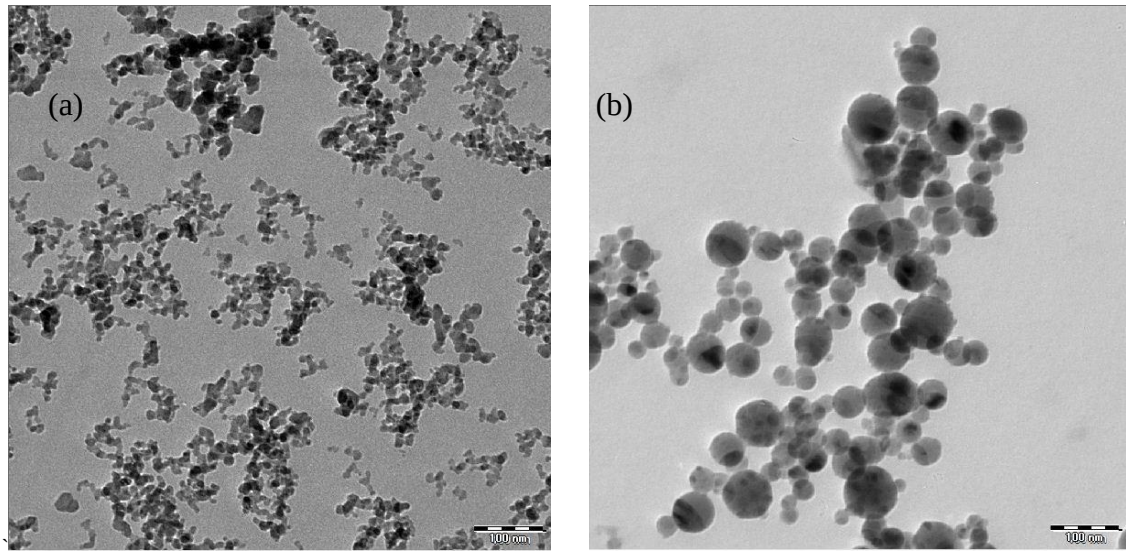

Figure 3.11: TEM images of (a) Alumina and (b) $TiSiO_4$ nanoparticles dispersed in water at 0.05% volumetric concentration

3.2 Experimental procedure

Once the experimental equipment have been installed and set up properly, tests can be started. Present experiment includes two main parts:

- Preparing the thermosyphon by filling the required amount of working fluid followed by vacuum pumping.
- Providing power to the heater and starting up the wickless thermosyphon.

At the first stage, the working fluids are prepared as mentioned before in a certain amount. The filling ratio of 1:1 (volume of fluid to the volume of the evaporator) was implemented for all the experimental runs. This means that a volume equal to the volume of the evaporator was prepared from the three fluids (distilled water, Al_2O_3/water, $TiSiO_4$/water). The fluid was inserted into the test section using a syringe and straw as depicted in Figure 3.12. It is mentionable that the thermosyphon was seen to be sensitive in terms of retaining the vacuum inside. Thus, filling was performed in such a cautious way. The straw was inserted all the way through the male connector and the hole in the vacuum valve to prevent any detrimental movement to the test rig. Besides, using a syringe could be a help in increasing the accuracy of the filling amount. A bolt was installed at the bottom of the thermosyphon to make it possible to evacuate the pipe from the inserted fluid. After removal of filling equipment, vacuum pump (EDWARDS oil sealed rotary vane pump as shown in Figure 3.13) was connected to the male connector and vacuuming was maintained for at least 30 minutes. This time is required to make sure that the heat pipe reaches the favorable negative pressure for proper functioning. To prevent any leakage, white tape was applied in all the joints and places prone to leakage. After vacuuming time was finished, the valve was closed and the pump was also removed before starting the next step of the experiment. First set of experiments were conducted by distilled water as the base line test.

The entire length of the thermosyphon was insulated by rock wool of 60 mm thickness to minimize the heat loss from heat pipe to the surroundings.

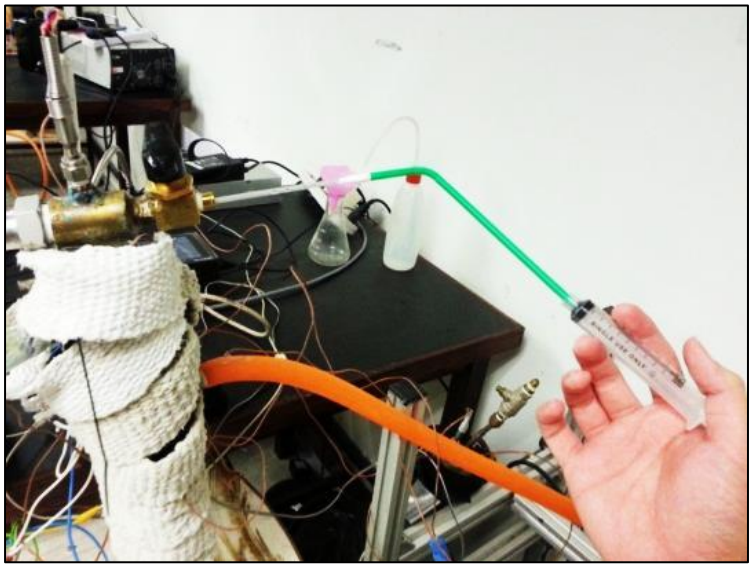

Figure 3.12: Filling the thermosyphon with the working fluid

Figure 3.13: Vacuum pump used to achieve the negative pressure inside the pump

After vacuuming process was finished, the main part of the experiment was commenced according to the following steps:

1. The thermocouples and pressure transmitter were installed as mentioned previously and they were linked to the data logger to record the temperature and pressure.

2. Water pump was then switched on to have the coolant water circulating around the condenser section at a designated flow rate. In order to maintain the inlet water temperature at the reservoir tank, the outgoing water was prevented from returning to the tank. The outlet water was then guided to drainage.
3. After making sure of the right position of band heaters, the power source was switched on to apply the input heat to the evaporator section. The power started from a value of 40W.
4. After around 40 minutes, steady-state operation was observed and the temperatures tended to remain unchanged. At this point, data logger was stopped and the input power was increased to 70W. Same procedure was repeated for input heat loads of 120W, 180W and 210 W.
5. When the experiments were finished for all input powers, thermosyphon was emptied from distilled water by opening the bolt at the bottom of the pipe. However, before injecting the new working fluid the heat pipe was put under vacuum drying (around 30 minutes) to prevent any mixing between new and current working fluid.

   The same procedure was implemented for Al_2O_3/water and $TiSiO_4$/water nanofluids at various prepared concentrations (0.01%, 0.02%, 0.05% and 0.075%). To see that the recorded data were free from any inherent flaws, the tests for each working fluid were repeated 3 times at the same conditions.

3.3 Data reduction

Important parameter that expresses the thermal performance of a thermosyphon is the overall thermal resistance which is represented by the ratio of temperature difference between evaporator and condenser to the heating load:

$$R_{th} = \frac{T_e - T_c}{P} \tag{3.4}$$

In order to investigate the changes in thermal performance, heat transfer coefficient at the evaporator will be calculated as well. The resistance to heat flow is associated with conduction through the wall in evaporator section (R_{we}) and boiling in evaporator inside the pipe (R_e). According to this notation, it can be outlined that:

For the evaporator:

$$P = \frac{T_e - T_{sat}}{R_{we} + R_e} \tag{3.5}$$

From the definition of above-mentioned thermal resistances, evaporator heat transfer coefficient can be calculated as follows:

$$h_e = \left[A_e \left(\frac{(T_e - T_{sat})}{P} - \frac{\ln\left(d_o / d_i\right)}{2\pi k_{wall} L_e} \right) \right]^{-1} \tag{3.6}$$

This parameter is important since it will be an indicator of heat transfer in the evaporator region. In most cases, thermosyphon is considered to have a good function if the heat transfer coefficient in the evaporator is as high as possible. Higher value for this parameter implies that boiling has taken place in a more vigorous way.

3.4 Uncertainty Analysis

The uncertainty of the experimental results was specified on the basis of deviations in different parameters involved in the experiment. The following equations were implemented to calculate the uncertainty for different mentioned parameters in this experiment (Holman, 2001):

$$\frac{\Delta P}{P} = \sqrt{\left(\frac{\Delta V}{V}\right)^2 + \left(\frac{\Delta I}{I}\right)^2} \tag{3.7}$$

$$\frac{\Delta R_{th}}{R_{th}} = \sqrt{(\frac{\Delta(T_e - T_c)}{(T_e - T_c)})^2 + (\frac{\Delta P}{P})^2} \tag{3.8}$$

$$\frac{\Delta h_e}{h_e} = \sqrt{\left(\frac{\Delta(T_e - T_{sat})}{(T_e - T_{sat})}\right)^2 + \left(\frac{\Delta P}{p}\right)^2} \tag{3.9}$$

The maximum uncertainty regarding the temperature measurements by thermocouples were 0.5°C. For both voltmeter and ammeter, maximum uncertainties of 0.25% were specified from the device manufacturer. The mass flow rate for water was measured directly by recording the time required to fill a 200 ml beaker with a precision of 5%. According to these values, a maximum uncertainty of 2.2% was calculated for the set of experiments in our study.

Chapter 4. Results and Discussion

To demonstrate the repeatability of the measured data in the experiment, typical recorded temperature distribution during three runs for the water-filled thermosyphon is displayed in Figure 4.1. To check if the tests were free from any flaws, different values for two input powers (40 W and 180 W) are drawn in the same graph along with the average values designated by the straight lines. As it can be observed, the deviation between readings is less than 1.7%. Attempts were made to ensure that the effective operating conditions such as water inlet temperature, mass flow rate and heat load remain constant to have a tangible comparison of the results.

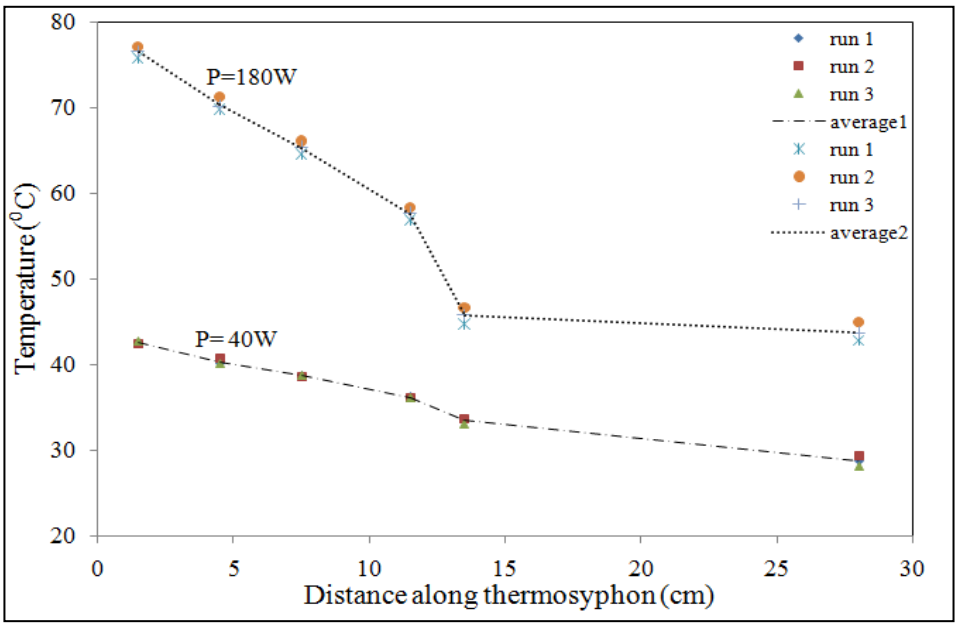

Figure 4.1: Repeatability of experiments for water-filled thermosyphon.

4.1 Effect of nanofluids on temperature distribution

Temperature distribution profiles in the two-phase closed thermosyphon are presented in Figure 4.2 for pure water and in Figure 4.3 and Figure 4.4 for the two nanofluids at 0.05 vol.%. On the right side of the graphs, the values of saturation, water inlet and

outlet temperatures are also brought. For all working fluids, the temperature decreases along the thermosyphon from evaporator to condenser. Appreciable reductions in the evaporator wall temperatures for the nanofluid-filled thermosyphon are observed in both cases compared with those for distilled water. For instance, at an input power of 40 W, wall temperatures in the evaporator (T_{e1}, T_{e2} and T_{e3}) reduced from 54.8^{0}C, 53.5^{0}C and 52.5^{0}C for distilled water to 42.5^{0}C, 40.5^{0}C and 38.7^{0}C for TiSiO4/water nanofluid. For the same power rating and thermocouple locations, 42.95^{0}C, 39.9^{0}C and 38.5^{0}C were recorded for Al_2O_3/water nanofluid. This behavior for nanofluids is true for other heat loads also, as seen from the figures. Simultaneously, the thermosyphon filled with nanofluids showed a slight rise in the condenser temperature. As a consequence, it can be outlined that using these two types of nanofluids cause a substantial reduction in the temperature difference between evaporator and condenser for the thermosyphon. Temperature distributions of other volumetric concentrations for both nanofluids are brought in Appendix A.

To compare the function of working fluids in high and low powers, temperature distributions are redrawn in Figure 4.5 for input powers of 40 W and 210 W. At low power, water induces highest wall temperature followed by Al_2O_3/water and $TiSiO_4$/water nanofluids both at 0.075 vol.%. When higher power (210 W) is exerted to the evaporator, Al_2O_3/water seems to exhibit the highest values for wall temperatures which implies the less efficiency of this nanofluid compared to the other two working fluids at high power. $TiSiO_4$/water, on the other hand, maintains its marked behavior in terms of diminishing the evaporator temperature. The highest condenser temperature is another noteworthy feature of this colloid compared to both water and alumina nanofluid at low and high heat loads. By this observation, it is signified that $TiSiO_4$/water boils at higher saturation temperature. This will induce less temperature

difference between the two sections and as a result a more flattened gradient along the device at this volumetric concentration.

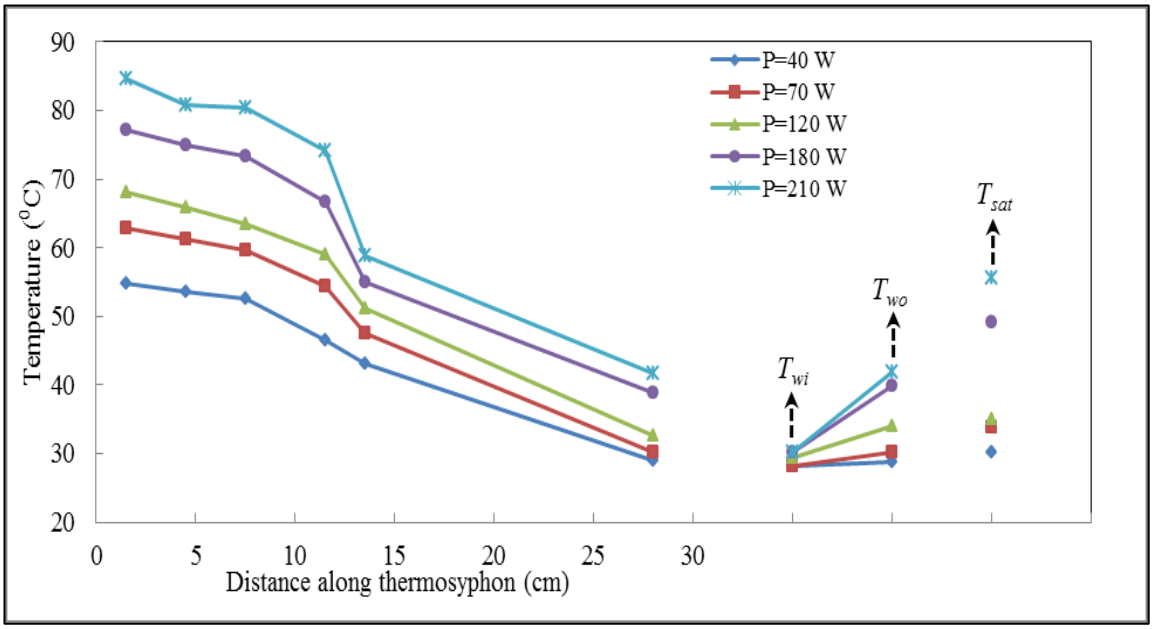

Figure 4.2: Temperature distribution along the thermosyphon filled with distilled water

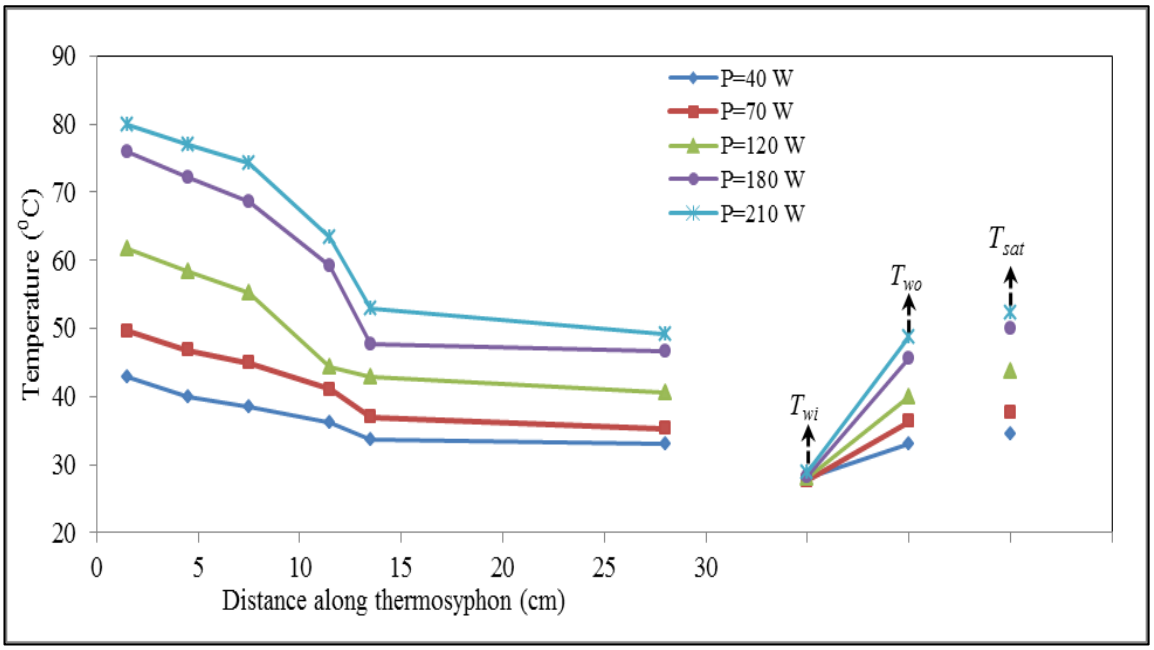

Figure 4.3: Temperature distribution along the thermosyphon filled with Al_2O_3/water nanofluid (0.05 vol.%)

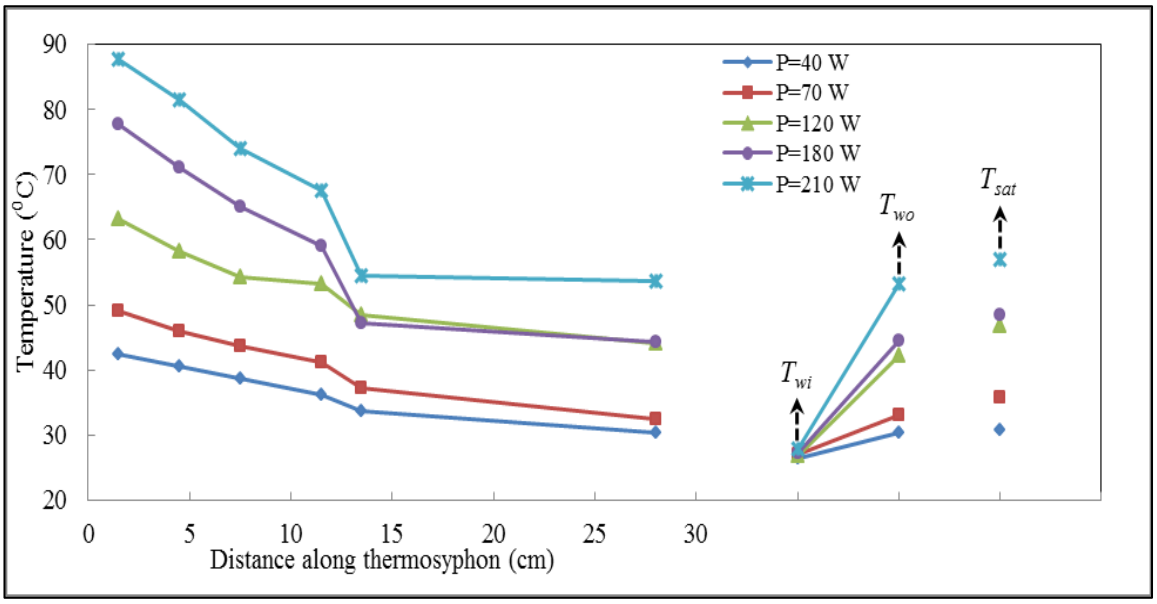

Figure 4.4: Temperature distribution along the thermosyphon filled with $TiSiO_4$/water nanofluid (0.05 vol%)

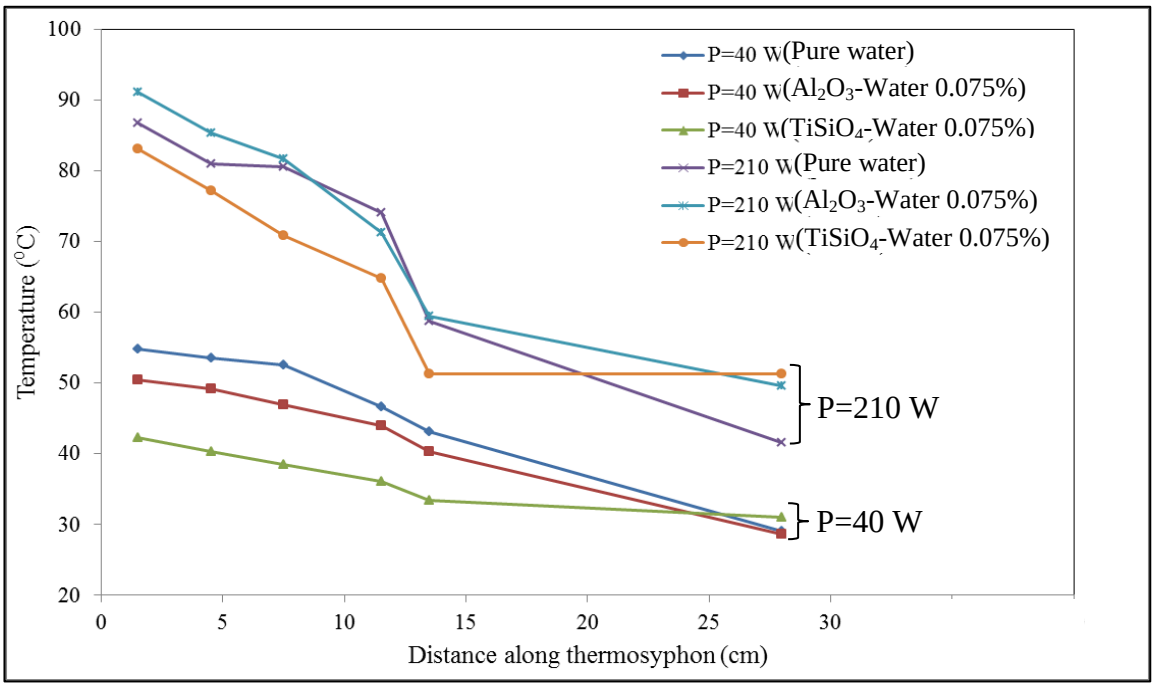

Figure 4.5: Comparison of temperature distribution between water and two nanofluids for 40 W and 210 W heat loads.

4.2 Effect of nanofluids on overall thermal resistance

Operating Temperature difference between evaporator and condenser is plotted against various input powers for Al_2O_3 (see Figure 4.6) and $TiSiO_4$ (see Figure 4.7) nanoparticles mixed with water as the basefluid for different concentrations. Temperature difference tends to rise with augmentation in heat inputs in the evaporator. As noted from these figures, water has higher temperature difference than the two nanofluids. At constant input heat, nanofluid absorbs more heat due to existence of nanoparticles. The increasing trend of temperature difference for the five powers is signified by regression equations in the figures.

To shed more light on the effect of nanofluids on the performance, thermal resistance of the wickless heat pipe is manifested in terms of different powers for various nanoparticle concentrations by Figure 4.8. The reduction in thermal resistance with the increase in input power is clearly noted from the figure. Besides, the influence of mixing nanoparticles with water is quite obvious for Al_2O_3/water nanofluid in Figure 4.8 (a) where for all concentrations and all powers resistance is decreased compared with pure water. For a certain heat load, thermal resistance drops significantly from pure water to a minimal value at 0.05% volume concentration and begins to rise again at the concentration of 0.075%. Other input powers also seem to share the same trend where the highest decrement in thermal resistance has taken place at 0.05 vol.%. For instance, at the power of 40 W, thermal resistance decreased substantially from 0.54 ^{0}C/W for distilled water to 0.18 ^{0}C/W for 0.05vol.% implying an almost 65% reduction in the resistance. However, this decrement was less remarkable for high powers. At an input power of 210 W, thermal resistance shows a 29% decrease from 0.187 ^{0}C/W for pure water to the minimum amount of 0.133 ^{0}C/W at 0.05 vol.% but increases again to 0.179^{0}C/W at 0.075 vol.%.

Figure 4.8 (b) exhibits a different behavior for $TiSiO_4$/water nanofluid, although thermal resistance is also lowered after implementing this nanofluid. For this nanofluid, at constant heat load, thermal resistance decreases with increments in particle concentration from 0.05 % to 0.075% where the lowest value for thermal resistance is achieved. Analogously, at lower power, more improvement is attained in the thermal performance of thermosyphon. A reduction of 57% in thermal resistance took place for input heat of 40 W when resistance changed from 0.54 ^{0}C/W for 0.05% vol.% to 0.23 ^{0}C/W for the concentration of 0.075%.For high power of 210 W, the acquired improvement in performance is about 34%. Accordingly, the optimum concentration for $TiSiO_4$/water nanofluid is found to be 0.075% unlike Al_2O_3/water nanofluid whose best performance turned out to be at lower volume concentration of 0.05%.

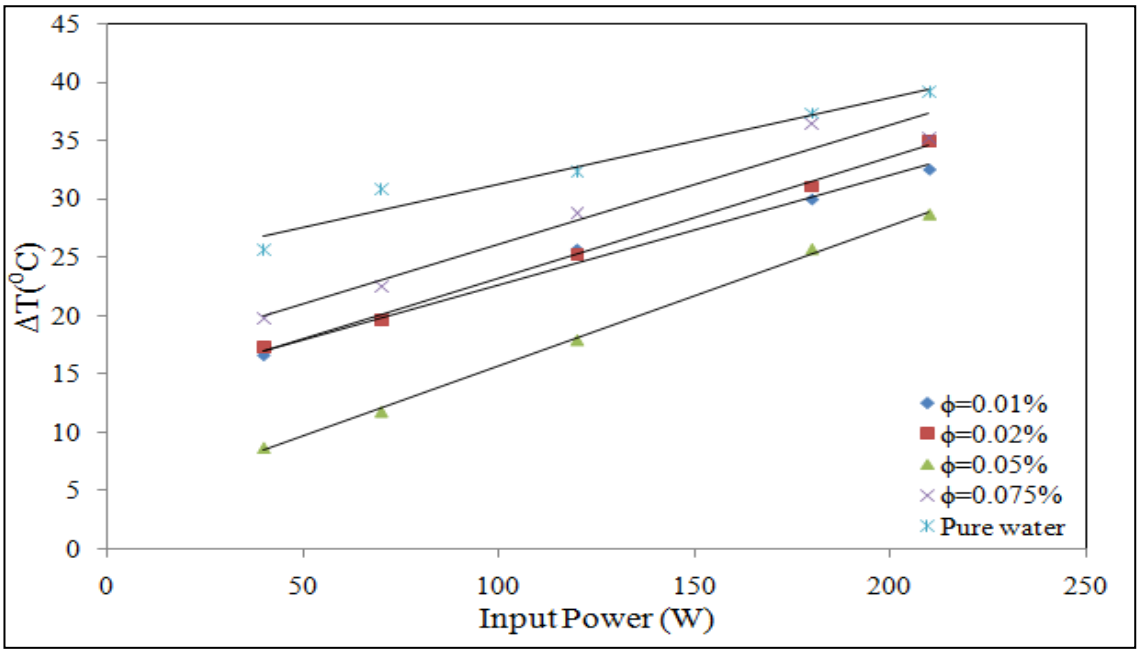

Figure 4.6: Operating Temperature difference Vs. input power (Al_2O_3/water nanofluid)

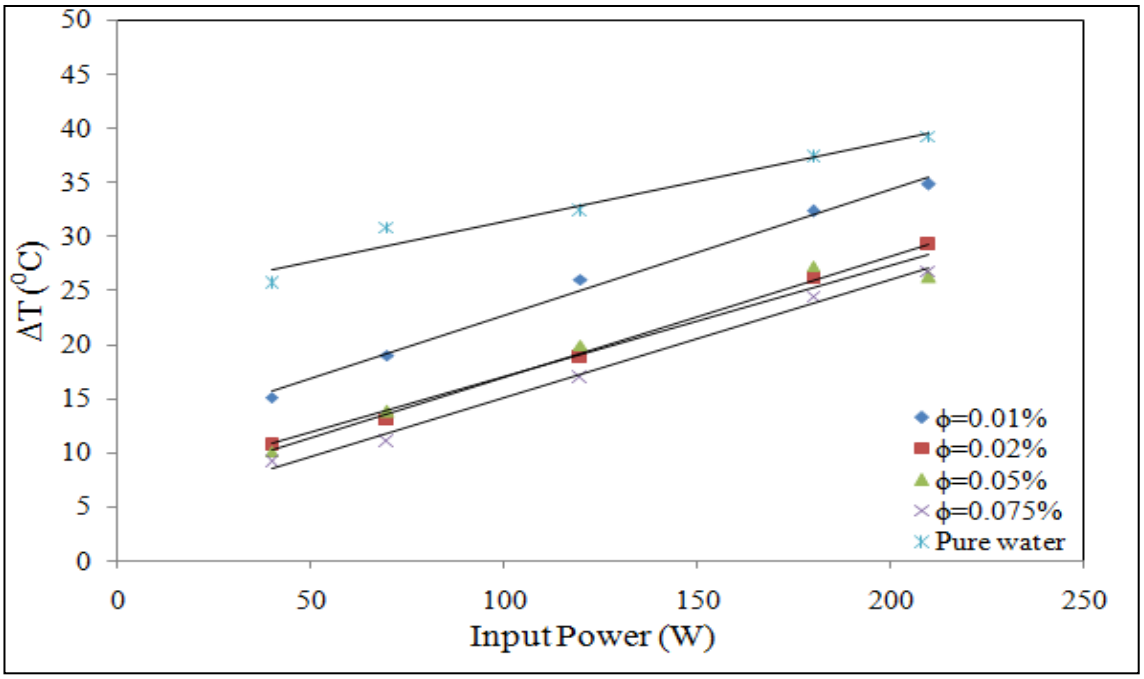

Figure 4.7: Operating Temperature difference Vs. input power ($TiSiO_4$/water nanofluid)

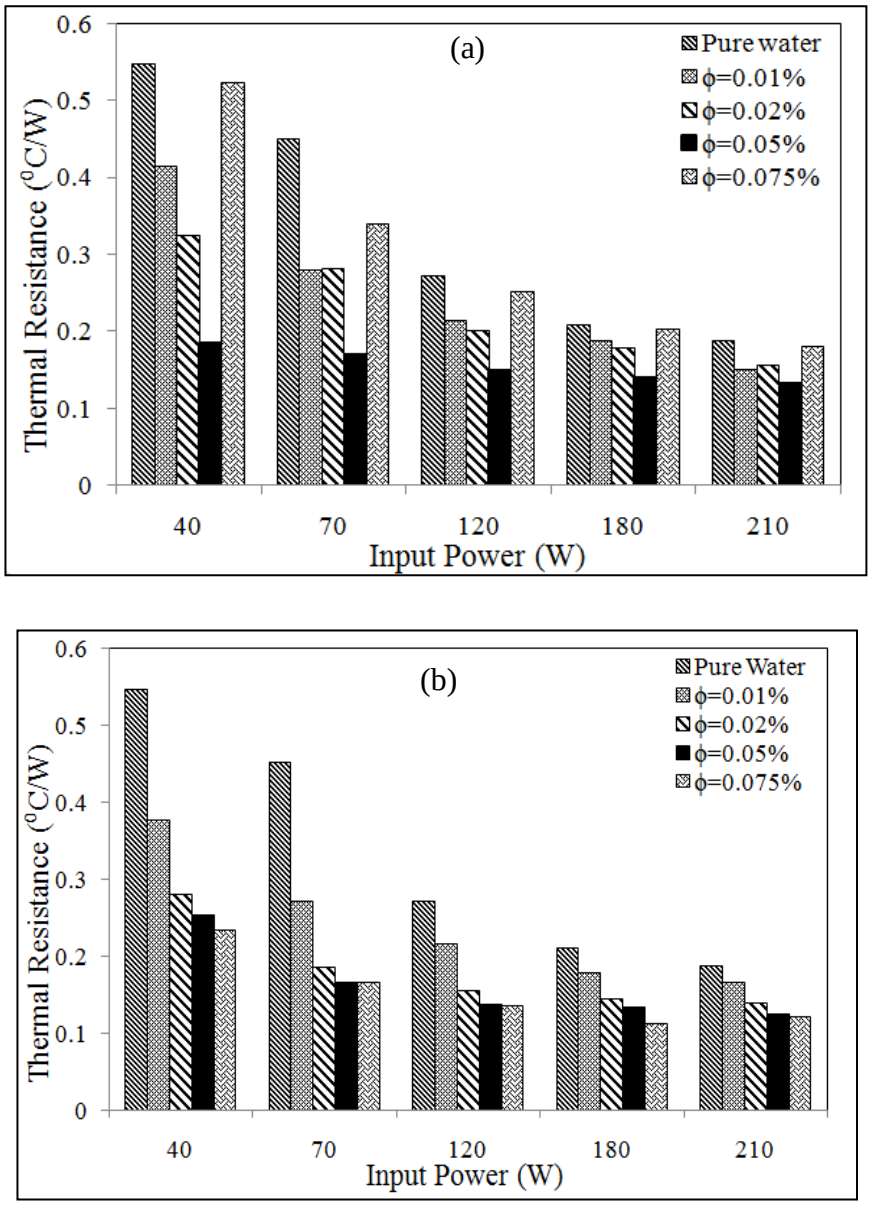

Figure 4.8: Overall thermal resistance of thermosyphon at different input powers for different concentrations of (a) Al_2O_3 and (b) $TiSiO_4$ nanoparticles.

4.3 Effect of nanofluids on evaporator heat transfer coefficient

The influence of dispersing nanoparticles on the evaporation inside the pipe is delineated through Figure 4.9 and Figure 4.10 for Al_2O_3/water and $TiSiO_4$/water nanofluids respectively. Experimental results indicate that both nanofluids have a generally increasing trend of boiling heat transfer coefficient with increments in the applied heat load. Compared with both nanofluids, water has the least evaporator heat

transfer coefficient which again is the evidence that existence of nanoparticles enhances the boiling coefficient for the thermosyphon. For Al_2O_3/water the maximum heat transfer coefficient belongs to the concentration of 0.05%. It is clearly depicted that at this optimum concentration, starting from 968 W/m^2 K at 40 W (compared with 324 W/m^2 K for water), the coefficient augments up to the maximum value of 1767 W/m^2 K at 210 W. On the other hand, in Figure 4.10 for $TiSiO_4$, it is noted that heat transfer coefficient increases all the way along with the increase in particle concentration. For this type of particle, maximum heat transfer occurs at the highest concentration of 0.075% with a value of 1753 W/m^2 K at 180 W. When the power reaches the maximum value, the effect of nanoparticles seem to be weakened as the difference between evaporation coefficients become minor. This fact implies that as the power grows, less improvement can be achieved by using nanofluids as the working fluid. Another feature of $TiSiO_4$/water nanofluid is that the increasing trend changes its behavior after input heat of 180 W. However, in Figure 4.9, heat transfer coefficient in the evaporator keeps on growing after 180 W for Al_2O_3/water nanofluid albeit the values are quite close with that of water at 210 W.

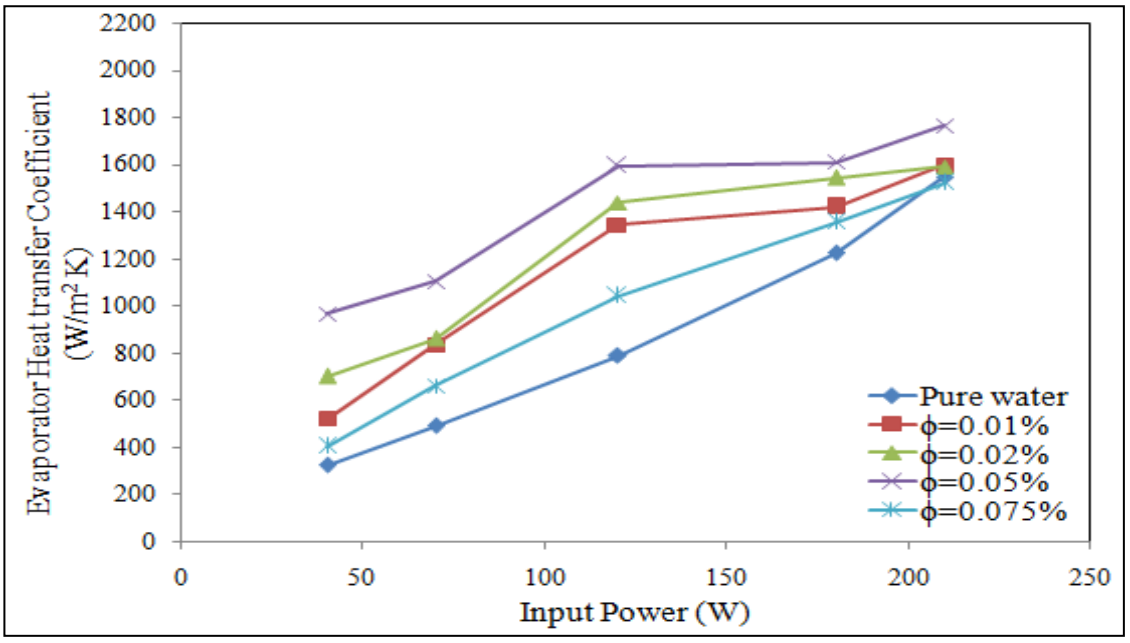

Figure 4.9: Evaporation heat transfer coefficient with respect to input power for different concentrations (Al_2O_3/water)

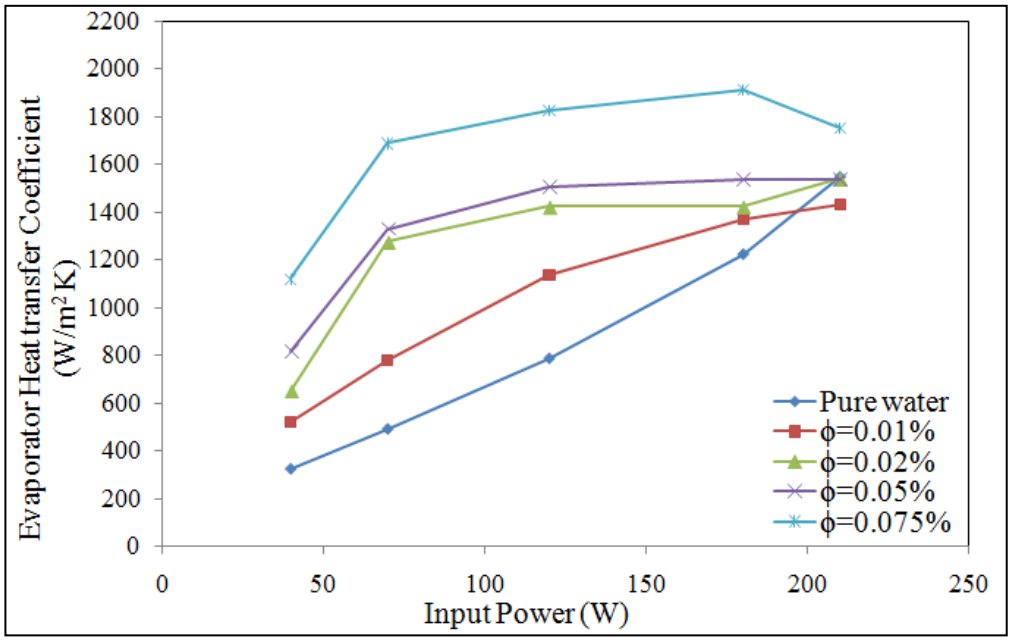

Figure 4.10: Evaporation heat transfer coefficient with respect to input power for different concentrations ($TiSiO_4$/water)

In order to expound the function of nanofluids in the current experiment, influence of nanoparticles on the boiling heat transfer should be investigated. This is due to the fact that the cooling ability of the thermosyphon is a result of phase change during boiling of

the working fluid in the evaporator section. Three reasons might be responsible for the special heat transfer characteristics of the nanofluid (Liu et al. (2010)): first enhancing the thermal conductivity of the suspension, second deposition of nanoparticles on the heating surface forming a porous layer that improves the surface wettability and finally the Brownian motion of nanoparticles which intensifies the turbulence. Higher thermal conductivity amends the functionality of a working fluid in a thermosyphon. Upon the addition of solid nanoparticles to a fluid, viscosity and densities will also increase. The relative effect of these three thermophysical properties on the performance of a thermosyphon can be investigated through the merit number defined by equation (4.1) (Reay and Kew (2006)). According to this parameter, enhancement of thermal conductivity can have more influence on the heat transfer characteristics of the thermosyphon. Larger values for merit number imply more suitability for the fluid.

$$M = \left(\frac{h_{fg} k_l^3 \sigma_l}{\mu_l} \right)^{\frac{1}{2}} \tag{4.1}$$

In addition, it has been outlined that as a consequence of microlayer evaporation beneath a vapor bubble(Collier and Thome (1996)), a porous layer is usually formed on the heating surface during boiling. To assure that this phenomenon also took place in our experiment, three copper pipes were subjected to pool boiling in three working fluids. Field Emission Scanning Electron Microscope (FESEM) images were then taken from the surface of the pipe and are presented in Figure 4.11. In parts (a) and (b) of this figure, the porous precipitate of nanoparticles is clearly distinguished compared with the case in part (c) where the pipe was boiled in pure water. This layer changes the boiling mechanism in two ways: not only by amplifying the roughness of the surface but with increasing the surface wettability and as a result the contact angle (Kim et al. (2007)). These can be in charge of changes in the behavior of nanofluids during boiling inside the thermosyphon in comparison with pure water. Stochastic movement of particles

known as Brownian motion might also impact the heat transfer rate especially in the vicinity of the pipe wall. The motion and fluctuation of nanoparticles near the surface will lead to more energy exchange which results in more heat transfer rate in the evaporator section.

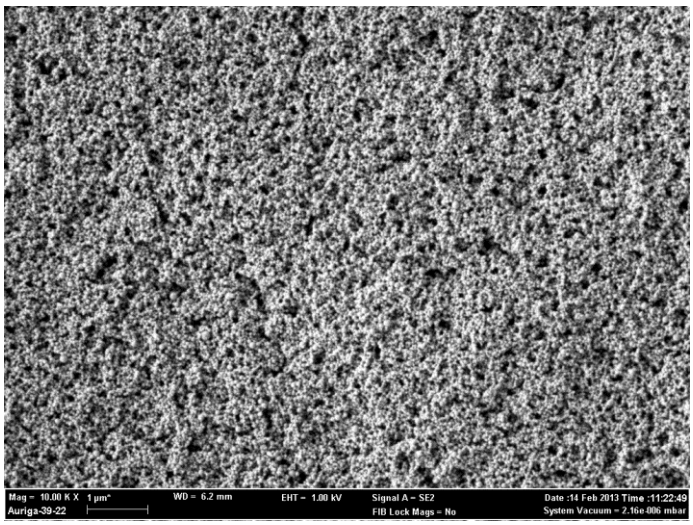

(a)

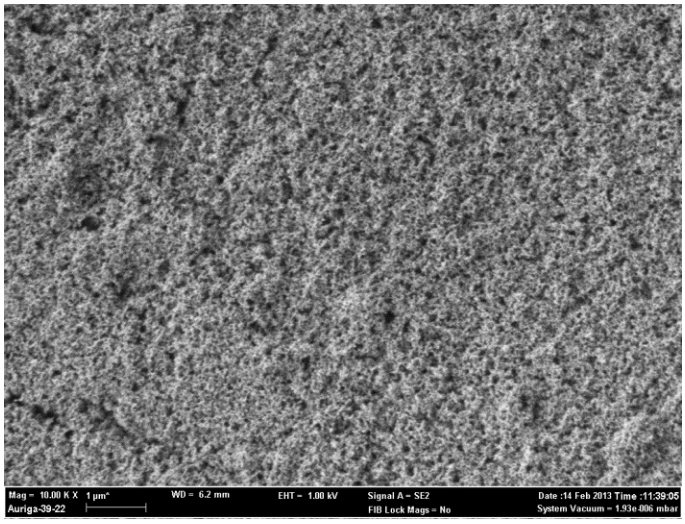

(b)

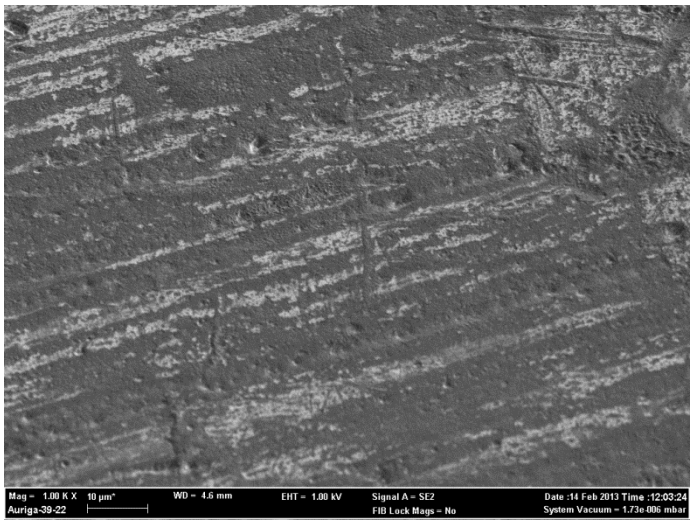

(c)

Figure 4.11: FESEM images of copper substrate boiled in (a) Al_2O_3/water nanofluid (0.05% vol. concentration) (b) $TiSiO_4$/water nanofluid (0.05% vol. concentration) (c) pure water.

The heat transfer characteristics of a thermosyphon operating with nanofluids depend on some parameters such as particle type, particle size, base fluid and bubble nucleation site. In the results, differences were detected between the function of Al_2O_3/water and TiSiO4/water nanofluids in terms of heat transfer rate and reduction in thermal resistance with change in volumetric concentration. As presented previously, an optimum concentration was discovered for alumina nanofluid while for $TiSiO_4$ mixed with water the heat transfer enhanced with increase in particle concentration. This might stem from the difference in size and shape of the particles. For $TiSiO_4$ nanoparticles, with a perfectly spherical shape, the increase in particle concentration intensifies the mentioned mechanisms of enhanced heat transfer. More volume fraction is along with more collision and particle-particle interaction. Another outcome of the rise in concentration is the bombardment of vapor bubbles by more particles. This phenomenon will create a situation where smaller nucleation size of vapor bubbles exist and less thermal resistance will deter heat transfer from solid surface to liquid. For Al_2O_3/water, on the other hand, the optimum thermal performance took place at the concentration of 0.05%. It is speculated that due to irregular shape and smaller size of these nanoparticles (as seen in Figure 3.11), the heat transfer tend to enhance up to a certain distribution (0.05%), but as the concentration gets further increased the trend changes. At higher concentrations for this nanoparticle, number of microcavities on the surface decreases gradually which is the reason behind reduction in active nucleation sites. This change will be a counter to enhancement of heat transfer by other mechanisms that will cause overall deterioration of thermal performance. However, direct measurement of nucleation site density on the surface is still lacking in the studies. This prevents a conclusive clarification of nanoparticle layer quality and boiling characteristics of alumina nanofluid. This is an area that requires additional study in future investigations.

Chapter 5. Conclusion and recommendation

5.1 Conclusions

The objective of this study was to examine the effects of using nanofluids on the performance of a two-phase closed thermosyphon through experiment. Different concentrations (0.01%, 0.02%, 0.05% and 0.075%) of Al_2O_3 as well as $TiSiO_4$ particles were dispersed in distilled water as base fluid. The research focused on the resulted changes in temperature distribution, overall thermal resistance of the thermosyphon and the heat transfer coefficient of the evaporator section. Various input powers (40-210 W) were applied in the evaporator to see the behavior of nanofluid-filled thermosyphon in low and high heat loads. After using the recorded data to analyze the results, the following conclusions can be deduced:

- Compared with pure water, both nanofluids showed lower temperature distribution along the heat pipe. According to temperature profiles, using nanoparticles flattens the temperature gradient which is a sign of improved heat transfer.
- Both nanofluids engender reductions in the overall thermal resistance of the thermosyphon. Reduction of up to 65% in thermal resistance was obtained for Al_2O_3/water. This reduction was measured to be 57% for $TiSiO_4$/water mixture. These observations imply that nanofluids improve the cooling ability of the thermosyphon.
- Evaporation heat transfer coefficient was also found to increase after using nanofluids. The relative enhancement in boiling heat transfer coefficient was more significant at low powers. For all working fluids, heat transfer coefficient increased with increase in the heat load.

- Volumetric concentration of nanoparticles plays a significant role on the function of nanofluids. For Alumina/water nanofluid biggest decrement in overall thermal resistance was achieved at 0.05 vol% while the optimum concentration for $TiSiO_4$/water was explored to be 0.075%. Although heat transfer coefficient improved by increasing particle concentration for $TiSiO_4$/water, it had the highest value at 0.05 vol.% for Al_2O_3/water showing a limit for increments in particle concentration.
- Surface imaging of a copper pipe proves that nanoparticles deposit on the surface, creating a porous layer that might be responsible for the different heat transfer behavior of nanofluids compared with pure water. Difference of particle type and size exert changes in behavior of nanofluids. This might be related to the surface morphology of the heated surface after boiling.
- Aside from nanoparticle precipitation, Brownian motion and increase of thermal conductivity cause enhancements in thermal performance.
- As a final verdict, using nanofluids as the working fluid in a two-phase closed thermosyphon has positive effects on the heat transfer characteristics. This capability influences the efficiency of the bigger system where the heat pipe is being used.

5.2 Recommendations

The concept of using nanofluids as coolants in heat pipes is still immature and requires further investigations. The preparation method of a nanofluid can majorly affect the stability and consequently the functionality of a nanofluid. Chemical reduction (single-step) method for preparation of nanofluids can be implemented to see the .new obtained thermophysical properties. This can alter the performance of a device such as thermosyphon that uses nanofluid as a coolant.

Upon enhancement in heat transfer, a thermosyphon with the same cooling ability but with smaller shape is possible to design. Measuring the reduction in size due to use of nanofluid can be a subject of future studies since it can affect the bulkiness of the whole system.

Long time ultrasonication of the nanofluid does not guarantee the prevention of agglomeration of particles. This might deter the mixture to function properly. Some techniques can be used to reduce the agglomeration. Functionalizing nanoparticles is one way. It will increase the stability and causes the nanoparticles to be well dispersed.

More accurate characterization of the heated surface after boiling can shed more light on the reason of heat transfer specification of a nanofluid. After particle deposition , number of active nucleation sites changes. Clear knowledge of the surface morphology can express the true nature of nanofluid boiling.

If the same nanofluids used in this study, are implemented in a heat pipe with wicked or grooved surface, they may show totally different results. Therefore other types of heat pipes (flat-shape, oscillating, etc.) can also be tested with these nanofluids.

References

Akbarzadeh, A., & Wadowski, T. (1996). Heat pipe-based cooling systems for photovoltaic cells under concentrated solar radiation. *Applied thermal engineering, 16*(1), 81-87.

Alizad, K., Vafai, K., & Shafahi, M. (2011). Thermal performance and operational attributes of the startup characteristics of flat-shaped heat pipes using nanofluids. *International Journal of Heat and Mass Transfer, 55*(1-3), 140-155.

Bang, I.C., & Heung Chang, S. (2005). Boiling heat transfer performance and phenomena of Al2O3–water nano-fluids from a plain surface in a pool. *International Journal of Heat and Mass Transfer, 48*(12), 2407-2419.

Buongiorno, J., Hu, L.W., & Truong, B.H. (2007). *Determination of pool boiling critical heat flux enhancement in nanofluids,* PhD Thesis, Massachusetts Institute of Technology.

Choi, S.U.S., & Eastman, J. (1995). Enhancing thermal conductivity of fluids with nanoparticles: Argonne National Lab., IL (United States).

Collier, J., & Thome, J. (1996). *Convective Boiling and Condensation* (3rd ed.). Oxford: Oxford Science Publications.

Coursey, J.S., & Kim, J. (2008). Nanofluid boiling: the effect of surface wettability. *International Journal of Heat and Fluid Flow, 29*(6), 1577-1585.

Das, S.K., Putra, N., & Roetzel, W. (2003). Pool boiling characteristics of nano-fluids. *International Journal of Heat and Mass Transfer, 46*(5), 851-862.

Do, K.H., Ha, H.J., & Jang, S.P. (2010). Thermal resistance of screen mesh wick heat pipes using the water-based Al2O3 nanofluids. *International Journal of Heat and Mass Transfer, 53*(25-26), 5888-5894.

Do, K.H., & Jang, S.P. (2010). Effect of nanofluids on the thermal performance of a flat micro heat pipe with a rectangular grooved wick. *International Journal of Heat and Mass Transfer, 53*(9-10), 2183-2192.

Eastman, J., Choi, S., Li, S., Yu, W., & Thompson, L. (2001). Anomalously increased effective thermal conductivities of ethylene glycol-based nanofluids containing copper nanoparticles. *Applied Physics Letters, 78*(6), 718-720.

Eastman, J., Choi, U., Li, S., Soyez, G., Thompson, L., & DiMelfi, R. (1999). Novel thermal properties of nanostructured materials. *Journal of Metastable and Nanocrystalline Materials, 2*, 629-634.

Grover, G., Cotter, T., & Erickson, G. (1964). Structures of very high thermal conductance. *Journal of applied physics, 35*(6), 1990-1991.

Holman, J.P. (2001). *Experimental methods for engineers* (7th ed.): McGraw-Hill.

Huminic, G., & Huminic, A. (2010). Heat transfer characteristics of a two-phase closed thermosyphons using nanofluids. *Experimental Thermal and Fluid Science, 35*(3), 550–557.

Huminic, G., Huminic, A., Morjan, I., & Dumitrache, F. (2011). Experimental study of the thermal performance of thermosyphon heat pipe using iron oxide nanoparticles. *International Journal of Heat and Mass Transfer, 54*(1), 656-661.

Jackson, J. (2007). *Investigation into the pool-boiling characteristics of gold nanofluids.* University of Missouri.

Kang, S.W., Wei, W.C., Tsai, S.H., & Yang, S.Y. (2006). Experimental investigation of silver nano-fluid on heat pipe thermal performance. *Applied thermal engineering, 26*(17), 2377-2382.

Khandekar, S., Joshi, Y.M., & Mehta, B. (2008). Thermal performance of closed two-phase thermosyphon using nanofluids. *International Journal of Thermal Sciences, 47*(6), 659-667.

Kim, S.J., Bang, I.C., Buongiorno, J., & Hu, L.W. (2007). Surface wettability change during pool boiling of nanofluids and its effect on critical heat flux. *International Journal of Heat and Mass Transfer, 50*(19–20), 4105-4116.

Lin, Y.H., Kang, S.W., & Chen, H.L. (2008). Effect of silver nano-fluid on pulsating heat pipe thermal performance. *Applied thermal engineering, 28*(11), 1312-1317.

Liu, Z., Xiong, J., & Bao, R. (2007). Boiling heat transfer characteristics of nanofluids in a flat heat pipe evaporator with micro-grooved heating surface. *International Journal of Multiphase Flow, 33*(12), 1284-1295.

Liu, Z., Yang, X., Wang, G., & Guo, G. (2010). Influence of carbon nanotube suspension on the thermal performance of a miniature thermosyphon. *International Journal of Heat and Mass Transfer, 53*(9-10), 1914-1920.

Liu, Z.H., Li, Y.Y., & Bao, R. (2010). Thermal performance of inclined grooved heat pipes using nanofluids. *International Journal of Thermal Sciences, 49*(9), 1680-1687.

Liu, Z.H., & Zhu, Q.Z. (2011). Application of aqueous nanofluids in a horizontal mesh heat pipe. *Energy Conversion and Management, 52*(1), 292-300.

Ma, H., Wilson, C., Borgmeyer, B., Park, K., Yu, Q., Choi, S., & Tirumala, M. (2006). Effect of nanofluid on the heat transport capability in an oscillating heat pipe. *Applied Physics Letters, 88*, 143116.

Maziuk, V., Kulakov, A., Rabetsky, M., Vasiliev, L., & Vukovic, M. (2001). Miniature heat-pipe thermal performance prediction tool–software development. *Applied thermal engineering, 21*(5), 559-571.

Mousa, M.G. (2011). Effect of nanofluid concentration on the performance of circular heat pipe. *Ain Shams Engineering Journal, 2*(1), 63-69.

Naphon, P., Assadamongkol, P., & Borirak, T. (2008). Experimental investigation of titanium nanofluids on the heat pipe thermal efficiency. *International Communications in Heat and Mass Transfer, 35*(10), 1316-1319.

Naphon, P., Thongkum, D., & Assadamongkol, P. (2009). Heat pipe efficiency enhancement with refrigerant-nanoparticles mixtures. *Energy Conversion and Management, 50*(3), 772-776.

Nemec, P., Čaja, A., & Malcho, M. (2013). Mathematical model for heat transfer limitations of heat pipe. *Mathematical and Computer Modelling, 57*(1-2), 126-136.

Noie-Baghban, S.H., & Majideian, G. (2000). Waste heat recovery using heat pipe heat exchanger (HPHE) for surgery rooms in hospitals. *Applied thermal engineering, 20*(14), 1271-1282.

Noie, S., Heris, S.Z., Kahani, M., & Nowee, S. (2009). Heat transfer enhancement using Al2O3/water nanofluid in a two-phase closed thermosyphon. *International Journal of Heat and Fluid Flow, 30*(4), 700-705.

Paramatthanuwat, T., Boothaisong, S., Rittidech, S., & Booddachan, K. (2010). Heat transfer characteristics of a two-phase closed thermosyphon using de ionized water mixed with silver nano. *Heat and mass transfer, 46*(3), 281-285.

Parametthanuwat, T., Rittidech, S., & Pattiya, A. (2010). A correlation to predict heat-transfer rates of a two-phase closed thermosyphon (TPCT) using silver nanofluid at normal operating conditions. *International Journal of Heat and Mass Transfer, 53*(21-22), 4960-4965.

Park, K.-J., & Jung, D. (2007). Boiling heat transfer enhancement with carbon nanotubes for refrigerants used in building air-conditioning. *Energy and Buildings, 39*(9), 1061-1064.

Putra, N., Septiadi, W.N., Rahman, H., & Irwansyah, R. (2012). Thermal performance of screen mesh wick heat pipes with nanofluids. *Experimental Thermal and Fluid Science, 40*, 10-17.

Qu, J., & Wu, H. (2011). Thermal performance comparison of oscillating heat pipes with SiO2/water and Al2O3/water nanofluids. *International Journal of Thermal Sciences, 50*(10), 1954-1962.

Qu, J., Wu, H., & Cheng, P. (2010). Thermal performance of an oscillating heat pipe with Al2O3-water nanofluids. *International Communications in Heat and Mass Transfer, 37*(2), 111-115.

Reay, D., & Kew, P.A. (2006). *Heat pipes: Theory, design and applications* (5th ed.): Butterworth Heinemann.

Riehl, R.R., & Santos, N. (2011). Water-copper nanofluid application in an open loop pulsating heat pipe. *Applied thermal engineering*.

Shafahi, M., Bianco, V., Vafai, K., & Manca, O. (2010a). An investigation of the thermal performance of cylindrical heat pipes using nanofluids. *International Journal of Heat and Mass Transfer, 53*(1-3), 376-383.

Shafahi, M., Bianco, V., Vafai, K., & Manca, O. (2010b). Thermal performance of flat-shaped heat pipes using nanofluids. *International Journal of Heat and Mass Transfer, 53*(7-8), 1438-1445.

Shanbedi, M., Zeinali Heris, S., Baniadam, M., Amiri, A., & Maghrebi, M. (2012). Investigation of Heat Transfer Characterization of EDA-MWCNT/DI-water Nanofluid in a Two-Phase Closed Thermosyphon. *Industrial & Engineering Chemistry Research, 51*(3), 1423–1428.

Shi, M., Shuai, M., Chen, Z., & Li, Q. (2007). Study on pool boiling heat transfer of nano-particle suspensions on plate surface. *Journal of Enhanced Heat Transfer, 14*(3).

Shin, D.R., Rhi, S.H., Lim, T.K., & Jang, J.C. (2011). Comparative study on heat transfer characteristics of nanofluidic thermosyphon and grooved heat pipe. *Journal of mechanical science and technology, 25*(6), 1391-1398.

Suman, B., De, S., & DasGupta, S. (2005). A model of the capillary limit of a micro heat pipe and prediction of the dry-out length. *International Journal of Heat and Fluid Flow, 26*(3), 495-505.

Teng, T.P., Hsu, H.G., Mo, H.E., & Chen, C.C. (2010). Thermal efficiency of heat pipe with alumina nanofluid. *Journal of Alloys and Compounds, 504*, S380-S384.

Tsai, C., Chien, H., Ding, P., Chan, B., Luh, T., & Chen, P. (2004). Effect of structural character of gold nanoparticles in nanofluid on heat pipe thermal performance. *Materials Letters, 58*(9), 1461-1465.

Wang, G.S., Song, B., & Liu, Z.H. (2010). Operation characteristics of cylindrical miniature grooved heat pipe using aqueous CuO nanofluids. *Experimental Thermal and Fluid Science, 34*(8), 1415-1421.

Wang, P.Y., Chen, X.J., Liu, Z.H., & Liu, Y.P. (2012). Application of nanofluid in an inclined mesh wicked heat pipes. *Thermochimica Acta, 593*, 100-108.

Wang, S., Lin, Z., Zhang, W., & Chen, J. (2009). Experimental study on pulsating heat pipe with functional thermal fluids. *International Journal of Heat and Mass Transfer, 52*(21), 5276-5279.

Wang, X., Xu, X., & Choi, S.U.S. (1999). Thermal conductivity of nanoparticle-fluid mixture. *Journal of Thermophysics and Heat Transfer, 13*(4), 474-480.

Wang, Y., & Vafai, K. (2000). An experimental investigation of the thermal performance of an asymmetrical flat plate heat pipe. *International Journal of Heat and Mass Transfer, 43*(15), 2657-2668.

Wannapakhe, S., Rittidech, S., Bubphachot, B., & Watanabe, O. (2009). Heat transfer rate of a closed-loop oscillating heat pipe with check valves using silver

nanofluid as working fluid. *Journal of mechanical science and technology, 23*(6), 1576-1582.

Wen, D. (2012). Influence of nanoparticles on boiling heat transfer. *Applied thermal engineering, 41*, 2-9.

Xue, H., Fan, J., Hu, Y., Hong, R., & Cen, K. (2006). The interface effect of carbon nanotube suspension on the thermal performance of a two-phase closed thermosyphon. *Journal of applied physics*, *100*, 104909.

Yang, X.F., & Liu, Z.H. (2011). Application of functionalized nanofluid in thermosyphon. *Nanoscale Research Letters, 6*(1), 494.

Yang, X.F., Liu, Z.H., & Zhao, J. (2008). Heat transfer performance of a horizontal micro-grooved heat pipe using CuO nanofluid. *Journal of Micromechanics and Microengineering*, *18*, 035038.

You, S., Kim, J., & Kim, K. (2003). Effect of nanoparticles on critical heat flux of water in pool boiling heat transfer. *Applied Physics Letters*, *83*, 3374.

Yu, W., & Choi, S. (2003). The role of interfacial layers in the enhanced thermal conductivity of nanofluids: a renovated Maxwell model. *Journal of Nanoparticle Research, 5*(1), 167-171.

Yulong, J., Corey, W., Hsiu-hung, C., & Hongbin, M. (2011). Particle shape effect on heat transfer performance in an oscillating heat pipe. *Nanoscale Research Letters*, *6*(1), 296.

Appendices

Appendix A

Temperature distribution along the thermosyphon for different concentrations of nanofluids

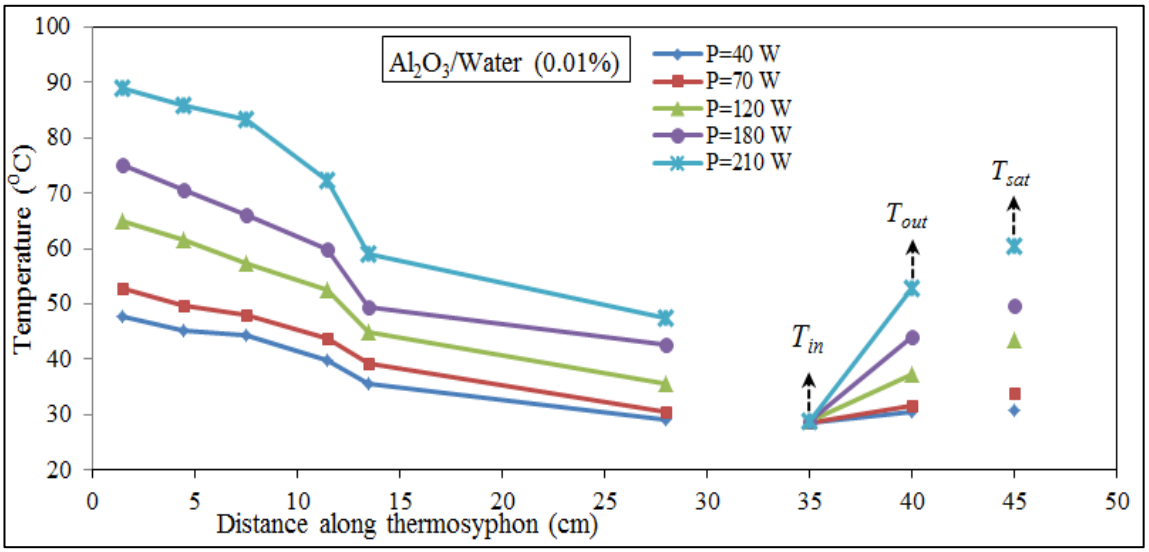

Figure A.1: Temperature distribution along the thermosyphon filled with Al_2O_3/water nanofluid (0.01 vol%)

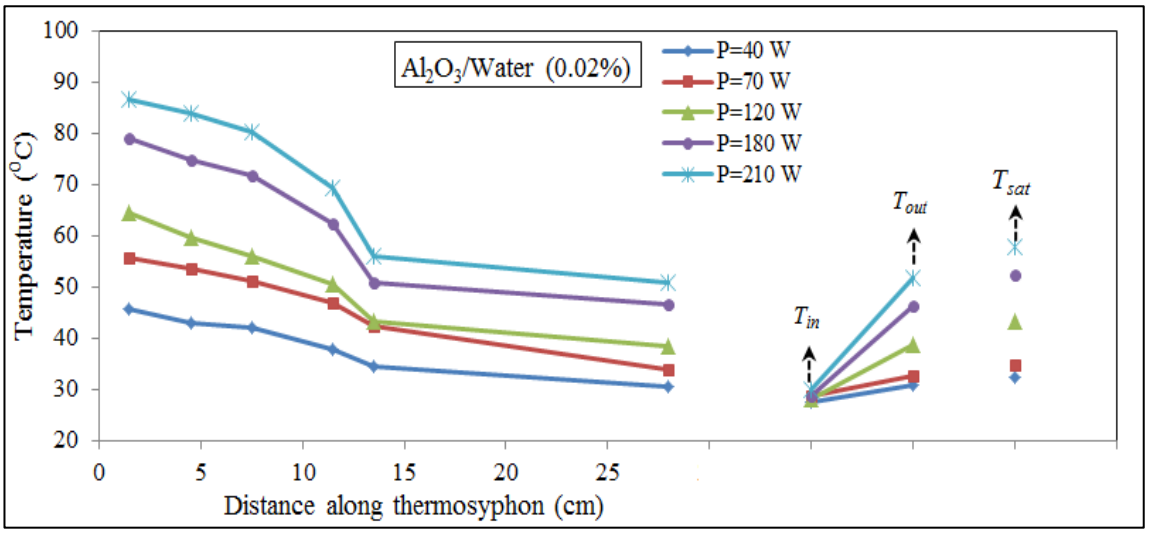

Figure A.2: Temperature distribution along the thermosyphon filled with Al_2O_3/water nanofluid (0.02 vol%)

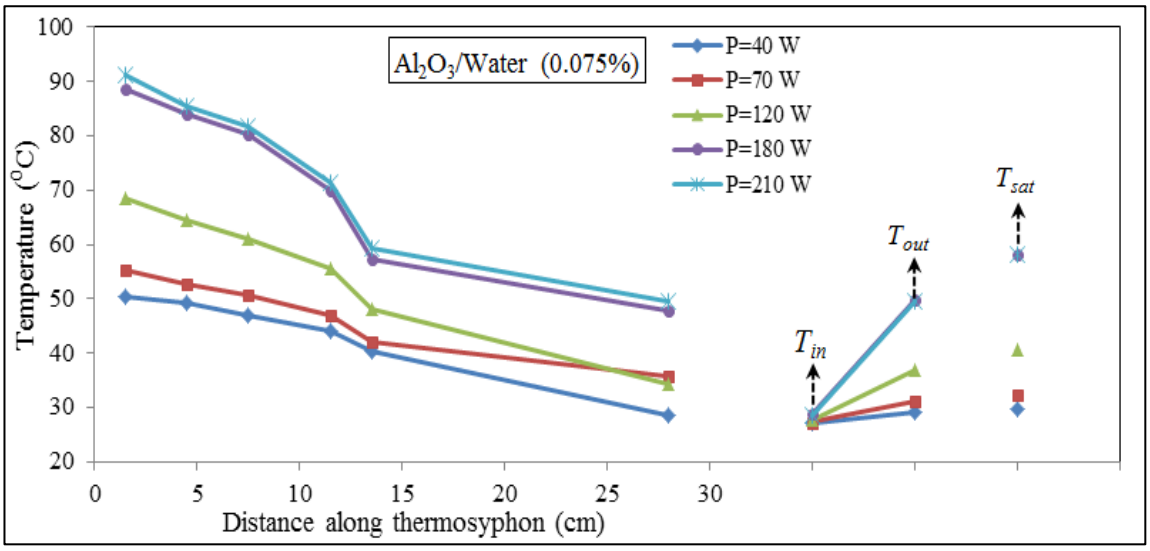

Figure A.3: Temperature distribution along the thermosyphon filled with Al_2O_3/water nanofluid (0.075 vol%)

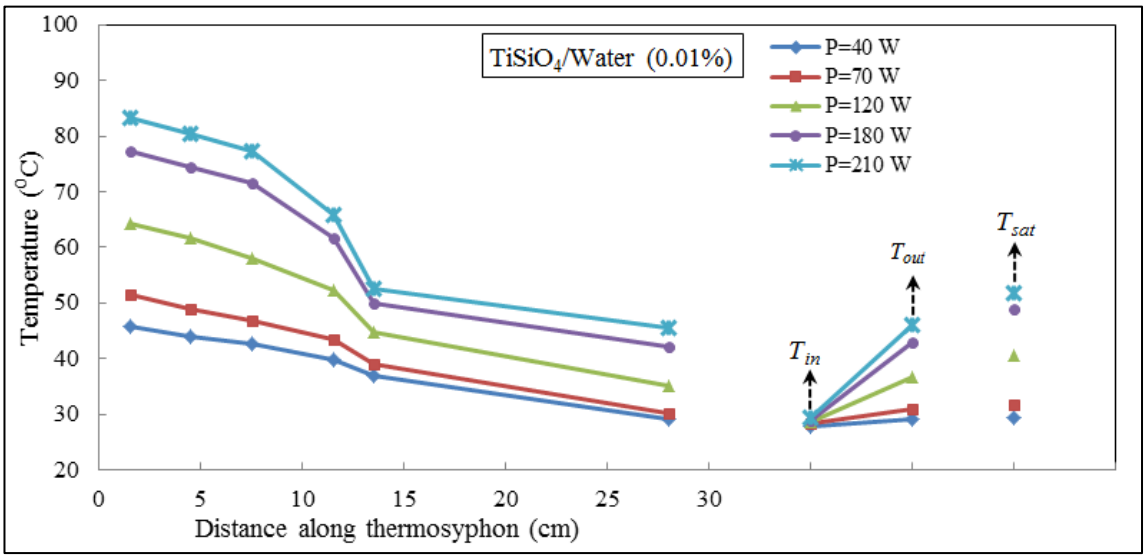

Figure A.4: Temperature distribution along the thermosyphon filled with $TiSiO_4$/water nanofluid (0.01 vol%)

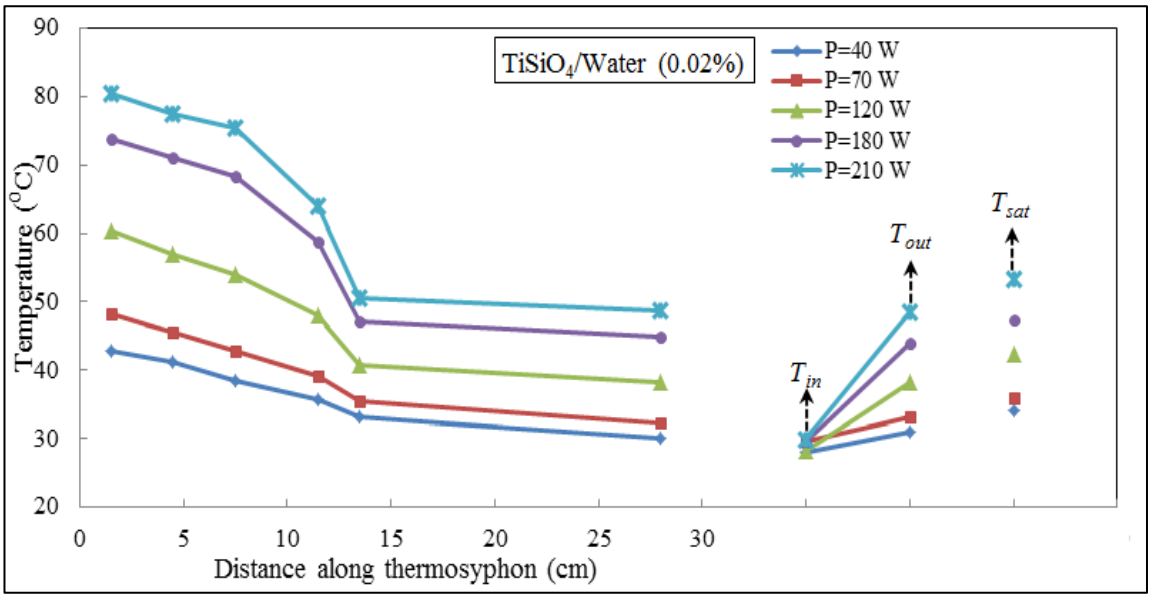

Figure A.5: Temperature distribution along the thermosyphon filled with $TiSiO_4$/water nanofluid (0.02 vol%)

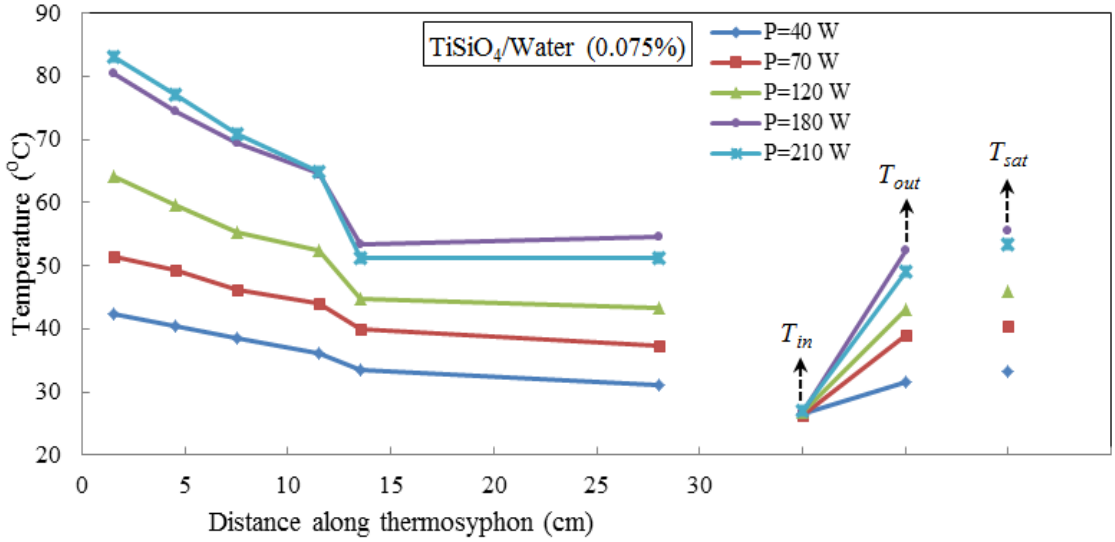

Figure A.6: Temperature distribution along the thermosyphon filled with $TiSiO_4$/water nanofluid (0.075 vol%)